Basic Research in Cardiology (2022) 117:5
https://doi.org/10.1007/s00395-022-00912-z

ORIGINAL CONTRIBUTION

Increased cytosolic calcium buffering contributes to a cellular arrhythmogenic substrate in iPSC-cardiomyocytes from patients with dilated cardiomyopathy

Philipp Jung[1,2] · Fitzwilliam Seibertz[1,2] · Funsho E. Fakuade[1,2] · Nadezda Ignatyeva[2,3] · Shrivatsan Sampathkumar[2,3] · Melanie Ritter[1,2] · Housen Li[4,5] · Fleur E. Mason[1,2] · Antje Ebert[2,3] · Niels Voigt[1,2,5]

Received: 14 June 2021 / Revised: 14 January 2022 / Accepted: 17 January 2022

Abstract

Dilated cardiomyopathy (DCM) is a major risk factor for heart failure and is associated with the development of life-threatening cardiac arrhythmias. Using a patient-specific induced pluripotent stem cell-derived cardiomyocyte (iPSC-CM) model harbouring a mutation in cardiac troponin T (R173W), we aim to examine the cellular basis of arrhythmogenesis in DCM patients with this mutation. iPSC from control (Ctrl) and DCM-TnT-R173W donors from the same family were differentiated into iPSC-CM and analysed through optical action potential (AP) recordings, simultaneous measurement of cytosolic calcium concentration ($[Ca^{2+}]_i$) and membrane currents and separately assayed using field stimulation to detect the threshold for AP- and $[Ca^{2+}]_i$-alternans development. AP duration was unaltered in TnT-R173W iPSC-CM. Nevertheless, TnT-R173W iPSC-CM showed a strikingly low stimulation threshold for AP- and $[Ca^{2+}]_i$-alternans. Myofilaments are known to play a role as intracellular Ca^{2+} buffers and here we show increased Ca^{2+} affinity of intracellular buffers in TnT-R173W cells, indicating increased myofilament sensitivity to Ca^{2+}. Similarly, EMD57033, a myofilament Ca^{2+} sensitiser, replicated the abnormal $[Ca^{2+}]_i$ dynamics observed in TnT-R173W samples and lowered the threshold for alternans development. In contrast, application of a Ca^{2+} desensitiser (blebbistatin) to TnT-R173W iPSC-CM was able to phenotypically rescue Ca^{2+} dynamics, normalising Ca^{2+} transient profile and minimising the occurrence of Ca^{2+} alternans at physiological frequencies. This finding suggests that increased Ca^{2+} buffering likely plays a major arrhythmogenic role in patients with DCM, specifically in those with mutations in cardiac troponin T. In addition, we propose that modulation of myofilament Ca^{2+} sensitivity could be an effective anti-arrhythmic target for pharmacological management of this disease.

Keywords iPSCs · Calcium handling · Cardiomyopathy · Ion channel · Action potential · Cardiovascular

Introduction

Dilated cardiomyopathy (DCM) represents the most common cardiomyopathy and is a major contributor to heart failure and sudden cardiac death [41]. Roughly, 40% of DCM

Philipp Jung and Fitzwilliam Seibertz contributed equally to this study.

✉ Antje Ebert
antje.ebert@med.uni-goettingen.de

✉ Niels Voigt
niels.voigt@med.uni-goettingen.de

1 Institute of Pharmacology and Toxicology, University Medical Center Göttingen, Robert-Koch-Straße 40, 37075 Göttingen, Germany

2 DZHK (German Center for Cardiovascular Research), Partner Site, Göttingen, Germany

3 Heart Research Center, Department of Cardiology and Pneumology, University Medical Center Göttingen, Robert-Koch-Straße 40, 37075 Göttingen, Germany

4 Institute for Mathematical Stochastics, Georg-August University, Göttingen, Germany

5 Cluster of Excellence "Multiscale Bioimaging: from Molecular Machines to Networks of Excitable Cells" (MBExC), University of Göttingen, Göttingen, Germany

Published online: 02 May 2022

cases are caused by inherited mutations, particularly in genes encoding for sarcomeric proteins [18, 42]. More than 50 disease-related genes have been identified, which also include mutations in cytoskeletal, mitochondrial and ion-channel proteins [41]. The lethal complications of DCM are largely due to the increased incidence of cardiac arrhythmias [33]. While previous work heavily focuses on the molecular basis of impaired contractile function, little is known about the mechanisms underlying cardiac arrhythmias in patients with DCM.

Human induced pluripotent stem cell-derived cardiomyocytes (iPSC-CM) are an emerging tool for modelling cardiac disease and for investigating the molecular basis of cardiac arrhythmias [25, 29, 44, 77]. The first mutation reported in a human patient-specific iPSC-CM model of dilated cardiomyopathy (DCM) was troponin T (TnT)-R173W [63]. Impaired calcium (Ca^{2+}) handling and reduced contractility are key features of patient-specific iPSC-CM carrying TnT-R173W [39, 63, 76]. Furthermore, it has been shown that TnT-R173W limits binding of protein kinase A to sarcomeric microdomains and attenuates consecutive phosphorylation of sarcomeric proteins such as troponin I (TnI) [9]. Since hypophosphorylation of TnI typically increases Ca^{2+} affinity of sarcomeric troponin C (TnC) [5, 60], it follows that Ca^{2+} buffering by myofilaments would be increased in DCM TnT-R173W iPSC-CM within a certain range of cytosolic Ca^{2+}, which can be visualised in the form of a buffer power curve [59].

Interestingly, increased myofilament Ca^{2+} sensitivity has been suggested to promote the occurrence of life-threatening arrhythmias in patients with familial hypertrophic cardiomyopathy (HCM) [1]. In particular, in mice with HCM-causing TnT mutations, the risk of developing ventricular arrhythmias was directly proportional to the degree of Ca^{2+} sensitisation caused by the mutation. We, therefore, hypothesise that a similar mechanism, i.e. increased Ca^{2+} binding to myofilaments, may also contribute to arrhythmogenesis in patients with DCM-causing TnT mutations.

Here, we utilised DCM patient-specific iPSC-CM carrying the TnT-R173W mutation (DCM-TnT-R173W iPSC-CM) to assess whether alterations in cellular Ca^{2+} handling and cellular electrophysiology may contribute to arrhythmogenesis in DCM patients harbouring mutations in TnT.

Materials and methods

Cardiac differentiation of human iPSC

Human induced pluripotent stem cells (iPSC) were grown to 80% confluence on Matrigel-coated plates using chemically defined E8 medium [8, 13] (Supplementary Fig. 1A) and were differentiated into beating iPSC-CM via a small molecule-based monolayer method, as described previously [12, 13, 34, 35]. From day 7, beating iPSC-CM could be observed. Following differentiation, human iPSC-CM were cultured in RPMI medium with B-27 Supplement (Life Technologies). TnT-R173W and Ctrl groups expressed regular levels of pluripotency markers in iPSC and cardiac markers in iPSC-CM, respectively (Supplementary Fig. 1). Following 25 days of cardiac differentiation, beating iPSC-CM monolayers were dissociated using TrypLE and plated onto Matrigel-coated glass coverslips (diameter 10 mm). Cells were investigated within a timeframe of 30–40 days after differentiation. Prior to experimentation, cells were loaded with 0.1 × VoltageFluor2.1Cl (Fluovolt, Thermo Scientific; 20 min loading) for Optical action potential (AP) analysis or 10 µM Fluo-3-acetoxymethyl ester (Fluo-3-AM, Thermo Scientific; 10 min loading, 50 min de-esterification) for intracellular Ca^{2+} investigation in a bath solution containing (in mM): $CaCl_2$ 2, Glucose 10, HEPES 10, KCl 4, $MgCl_2$ 1, NaCl 140, Probenecid 2; pH = 7.35 adjusted with NaOH. All protocols were approved by the Ethics Committee of the University Medical Center Göttingen (No. 10/9/15 and 15/2/20). Informed consent was obtained from all participants and all research was performed in accordance with relevant guidelines and regulations.

Electrical field stimulation of iPSC-CM

Coverslips containing iPSC-CM were transferred to a 37 ± 0.5 °C heated chamber containing bath solution. Cells were electrically stimulated at increasing frequencies (0.5 Hz, 1 Hz, 2 Hz, 3 Hz, 4 Hz and 5 Hz) with two parallel platinum electrodes connected to an external stimulator (IonOptix Myopacer cell stimulator). Stimuli were set to 3–5 ms bipolar pulses with voltages ~ 25% above the contraction threshold (normally between 10 and 30 V). APs were recorded from isolated masked cells on the stage of an epifluorescence microscope (λ_{Ex} = 470 nm, λ_{Em} = 535 nm), which was optimised for high-speed signal capture with a photomultiplier as previously described [52, 58]. Three APs from each cell at every measured frequency were ensemble averaged for offline analysis of AP parameters with Clampfit 10.7 (Molecular Devices). Whole-trace AP alternans magnitude was analysed using a discrete Fourier transform-based spectral method as described previously [15, 50]. Cytosolic Ca^{2+} levels were estimated as a change in fluorescence intensity relative to the resting fluorescence intensity at the beginning of each experiment ($\Delta F/F_0$).

Patch-clamp and simultaneous intracellular Ca^{2+} measurements

Coverslips containing iPSC-CM were transferred to a 37 ± 0.5 °C heated chamber and were superfused with bath

solution containing (in mM): 4-aminopyridine 5, $BaCl_2$ 0.1, $CaCl_2$ 2, Glucose 10, HEPES 10, KCl 4, $MgCl_2$ 1, NaCl 140, Probenecid 2; pH = 7.35 adjusted with NaOH. Simultaneous measurements of membrane currents and intracellular Ca^{2+} were performed under voltage-clamp using the whole-cell ruptured-patch configuration. Membrane currents were measured and analysed using pClamp-Software (V 10.7 Molecular Devices). Fluo-3 pentapotassium salt, 0.1 mM (Thermo Scientific) was added to the pipette solution containing (in mM): EGTA 0.02, GTP-Tris 0.1, HEPES 10, K-aspartate 92, KCl 48, Mg-ATP 1, Na_2-ATP 4; pH = 7.2 adjusted with KOH. Tip resistances of borosilicate glass microelectrodes were 3–7 MΩ. A voltage-clamp protocol using a holding potential of − 80 mV and a 100 ms voltage step to +10 mV at 0.5 Hz was employed to activate L-type Ca^{2+} current ($I_{Ca,L}$) and corresponding triggered Ca^{2+} transients. A 100 ms ramp pulse to − 40 mV to inactivate the fast Na^+ current was applied before each depolarising step. Membrane capacitance measurements were acquired and current was expressed as current density (pA/pF).

To quantify intracellular Ca^{2+} concentration ($[Ca^{2+}]_i$), Fluo-3 was excited at 488 nm and emitted light (> 520 nm) converted to $[Ca^{2+}]_i$, assuming

$$[Ca^{2+}]_i = k_d\left(\frac{F}{F_{max} - F}\right),$$

where k_d is the dissociation constant of Fluo-3 (864 nM), F is the Fluo-3 fluorescence; F_{max} is the Ca^{2+}-saturated fluorescence obtained at the end of each experiment [70, 71]. Ca^{2+} transients were analysed by averaging 10 consecutive traces. Sarcoplasmic reticulum (SR) Ca^{2+} content and Ca^{2+} buffering were quantified as previously described by the application of high concentration caffeine (10 mM) [10, 14, 59, 66].

Measurements of Ca^{2+} fluxes (integrated $I_{Ca,L}$) and SR Ca^{2+} content (integrated I_{NCX}) are expressed per litre total cell volume, which has been estimated based on a capacitance to volume relationship of 4.57 pF/pL [21].

Statistical analysis

Summarised data are reported as mean ± SEM, unless otherwise specified. Clustering of experimental data within separate differentiations was tested in 6 WT differentiations and appeared to be negligible (Supplementary Fig. 2). Continuous data with a sample size $n \geq 30$ were assumed to be normally distributed (central limit theorem) [28]. Values with a distribution between $n = 10$–30 were tested for normality using the Shapiro–Wilk test. Normally distributed data were compared using unpaired two-tailed Student's t test. Non-normally distributed data and all data sets with n < 10 were compared using the Mann–Whitney U test, as indicated in the figure legends. Kaplan–Meier curve data were compared using the Gehan–Breslow–Wilcoxon test. A P value < 0.05 was considered to be statistically significant.

Results

Action potential alternans in DCM-TnT-R173W iPSC-CM

We first assessed optical AP characteristics of isolated iPSC-CM from DCM patients carrying the cardiac troponin T mutation (R173W) and control iPSC-CM from the same family (Ctrl). iPSC-CM were stimulated at a range of frequencies using electrical field stimulation. AP duration at 90% repolarisation (APD_{90}) was not significantly different between both groups (Fig. 1A, B, 0.5 Hz: APD_{90} R173W: 171 ± 19.6, n/N = 16/3 vs. Ctrl: 156 ± 21.4 ms, n/N = 11/3). In addition, post-rest potentiation was not enhanced in R173W cells (Supplementary Fig. 3A, B) [57]. AP restitution, describing the relationship between APD and the previous diastolic interval, was also unchanged. Neither group produced a curve with a maximal slope greater than 1 (Fig. 1B). A maximal slope of 1 or greater is assumed to be a pre-requisite for the development of action potential-driven alternans, a phenomenon describing beat-to-beat variation in AP morphology [51, 73]. Despite this, AP alternans was observed at higher frequencies in DCM-TnT-R173W iPSC-CM, and was almost absent in Ctrl iPSC-CM (Fig. 1C, D). A discrete Fourier transform spectral analysis revealed a higher incidence of alternans during both phase 0–1 and phase 2–3 of an action potential event (Supplementary Fig. 3C, D).

Ca^{2+} alternans in DCM-TnT-R173W iPSC-CM

It has been shown previously that DCM-TnT-R173W iPSC-CM are characterised by impaired systolic contractility and slowed diastolic relaxation [9], with the latter pointing to impaired diastolic Ca^{2+} removal from the cytosol [39]. Impaired diastolic Ca^{2+} homeostasis has been shown to contribute to Ca^{2+}-driven alternans and, therefore, represent a major mechanism of cardiac arrhythmias. To further investigate diastolic Ca^{2+} handling and potential arrhythmogenic mechanisms, Fluo-3-loaded DCM-TnT-R173W iPSC-CM were stimulated at 0.5 Hz using electrical field stimulation. Representative normalised traces are shown in Fig. 2A (upper panel). Similar to previous studies [9, 39, 63], DCM-TnT-R173W iPSC-CM showed delayed Ca^{2+} transient time-to-peak values (Supplementary Fig. 4A). The time constant of decay was quantified by fitting a single exponential curve to the decay phase of the transient (from 90 to 10% of the amplitude). The time constant of decay was higher in DCM-TnT-R173W iPSC-CM (Fig. 2B), suggesting slower Ca^{2+}

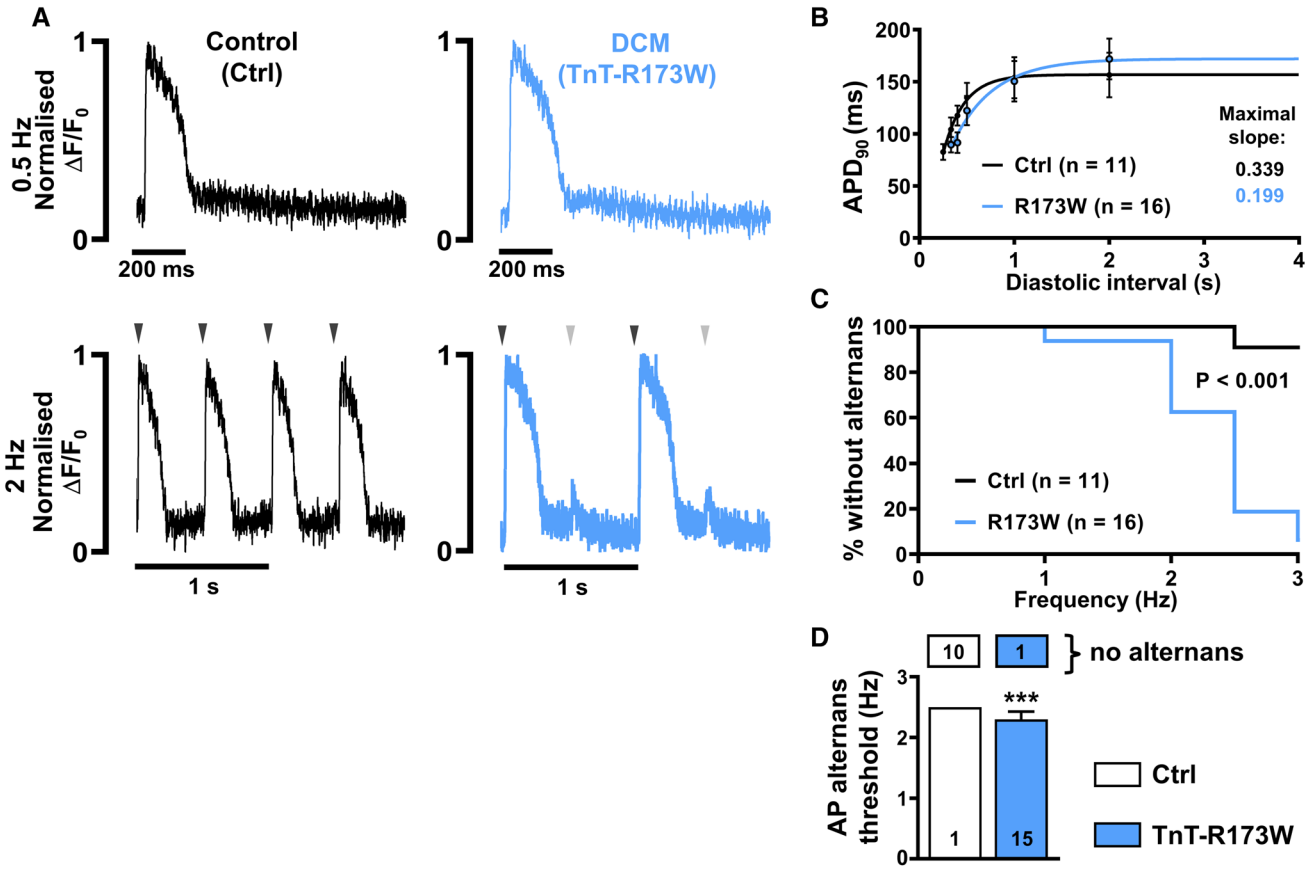

Fig. 1 Incidence of action potential (AP) alternans in control (Ctrl) and DCM-TnT-R173W induced pluripotent stem cell-derived cardiomyocytes (iPSC-CM). **A** Normalised representative traces of optical AP at 0.5 Hz (upper) and 2 Hz (lower) in Ctrl (left) and TnT-R173W (right) iPSC-CM. Arrowheads indicate electrical stimulation and illustrate when beat-to-beat alterations are present. **B** Action potential duration at 90% repolarisation (APD_{90}) at increasing diastolic intervals (AP restitution) fitted with a one-phase association nonlinear function to determine maximum curve slope. **C** Kaplan–Meier plot showing the percentage of cells without alternans in relation to the respective pacing frequency. **D** Alternans threshold frequency. Number of myocytes without AP alternans is shown in boxes above. *n* = number of iPSC-CM from three batches. Data are mean ± SEM. ***$P < 0.001$ using the Mann–Whitney *U* test (**D**) and Gehan–Breslow–Wilcoxon test (**C**)

removal from the cytosol, which is hypothesised to predispose the cardiomyocyte to the occurrence of Ca^{2+} transient alternans, i.e. beat-to-beat alterations of systolic Ca^{2+} transient amplitude [15, 73].

The occurrence of Ca^{2+} transient alternans in DCM-TnT-R173W iPSC-CM was investigated by increasing stimulation frequency stepwise up to 5 Hz (Fig. 2A). Strikingly, at 5 Hz, Ca^{2+} transient alternans was observed in all DCM-TnT-R173W iPSC-CM but only in 47% of Ctrl iPSC-CM. Kaplan–Meier analysis of alternans occurrence over the whole range of frequencies revealed significantly higher susceptibility to Ca^{2+} transient alternans in R173W-mutant cells. In addition, the threshold for Ca^{2+} transient alternans, i.e. mean frequency at which alternans first occurs, was significantly lower in the DCM-TnT-R173W group (Fig. 2C). Taken together, DCM-TnT-R173W iPSC-CM show slower Ca^{2+} removal from the cytosol, which may contribute to the occurrence of arrhythmogenic alternans in DCM patients harbouring this mutation.

Smaller amplitude of $I_{Ca,L}$-triggered Ca^{2+} transient in TnT-R173W iPSC-CM

To further investigate mechanisms underlying impaired Ca^{2+} handling in DCM-TnT-R173W iPSC-CM, epifluorescence was combined with the whole-cell voltage-clamp technique. No significant difference between membrane capacitance of DCM-TnT-R173W and Ctrl iPSC-CM was observed (R173W: 21.65 ± 1.63 pF, n/N = 46/5 vs. Ctrl: 27.38 ± 3.28 pF, n/N = 29/3; Mann–Whitney: $P = 0.33$), indicating comparable cell size. $I_{Ca,L}$ was induced by a voltage-step protocol (0.5 Hz stimulation frequency) and was measured simultaneously with cytosolic Ca^{2+} (Fig. 3A).

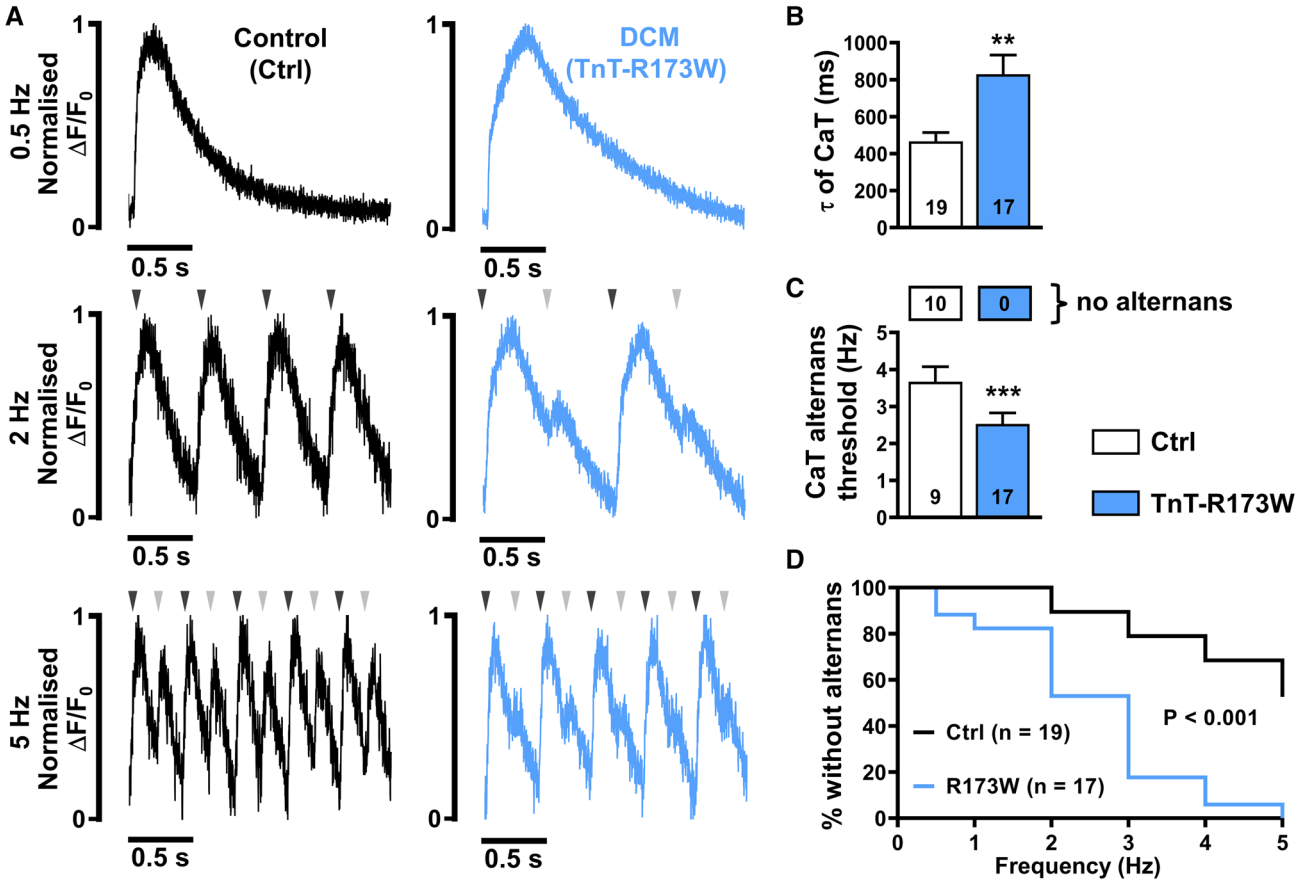

Fig. 2 Incidence of Ca^{2+} alternans in control (Ctrl) and DCM-TnT-R173W induced pluripotent stem cell-derived cardiomyocytes (iPSC-CM). **A** Normalised representative traces of Ca^{2+} transients (CaT) at 0.5 Hz (upper), 2 Hz (middle) and 5 Hz (lower) in Ctrl (left) and TnT-R173W (right) iPSC-CM. Arrowheads indicate electrical stimulation and illustrate when beat-to-beat alterations are present. **B** Ca^{2+} transient time constant of decay (τ). **C** Alternans threshold frequency. Number of myocytes without CaT alternans is shown in boxes above. **D** Kaplan–Meier plot showing the percentage of cells without alternans in relation to the respective pacing frequency. n = number of iPSC-CM from three batches. Data are mean ± SEM. $^{**}P < 0.01$ and $^{***}P < 0.001$ vs. Ctrl using Student's t test (**B**), Mann–Whitney U test (**C**) and the Gehan–Breslow–Wilcoxon test (**D**)

The peak amplitude and integral of $I_{Ca,L}$ were both greater in DCM-TnT-R173W, compared to Ctrl. Interestingly, despite greater $I_{Ca,L}$, the triggered Ca^{2+} transient amplitude was smaller in DCM-TnT-R173W compared to Ctrl (Fig. 3C right panel). Diastolic Ca^{2+} levels were comparable in both groups (Fig. 3C left panel).

Increased intracellular Ca^{2+} buffering in DCM-TnT-R173W iPSC-CM

The Ca^{2+} transient amplitude is determined by various factors such as $I_{Ca,L}$ and SR Ca^{2+} content. Considering increased $I_{Ca,L}$ (Fig. 3B), we subsequently measured SR Ca^{2+} content. After 3–5 min stimulation at 0.5 Hz using the voltage-step protocol described above, myocytes were clamped at − 80 mV and caffeine (10 mM) was applied to induce complete Ca^{2+} release from the SR (Fig. 3D upper panel). The amplitude of the resulting caffeine-induced Ca^{2+} transient was smaller in DCM-TnT-R173W, compared to Ctrl (Fig. 3E).

As the majority of Ca^{2+} released from the SR during caffeine application is extruded out of the cell by the electrogenic Na^{+}-Ca^{2+}-exchanger (NCX), integration of the resulting NCX current can be used as an index of the "total" amount of Ca^{2+} released from the SR. This was comparable in DCM-TnT-R173W and Ctrl (Fig. 3D middle panel, F), in contrast with the amplitude of the caffeine-induced Ca^{2+} transient, which was smaller in DCM-TnT-R173W. Since the latter is quantified using intracellular Ca^{2+} indicators such as Fluo-3, and intracellular Ca^{2+} buffers such as SR Ca^{2+}-ATPase (SERCA) and TnC compete with the indicator for binding to Ca^{2+} ions, the caffeine-induced Ca^{2+} transient represents only the "free" cytosolic Ca^{2+} concentration [59]. Therefore, an increase in intracellular Ca^{2+} buffering may explain the reduced amplitude of the caffeine-induced Ca^{2+} transient, despite comparable measurements of total Ca^{2+}.

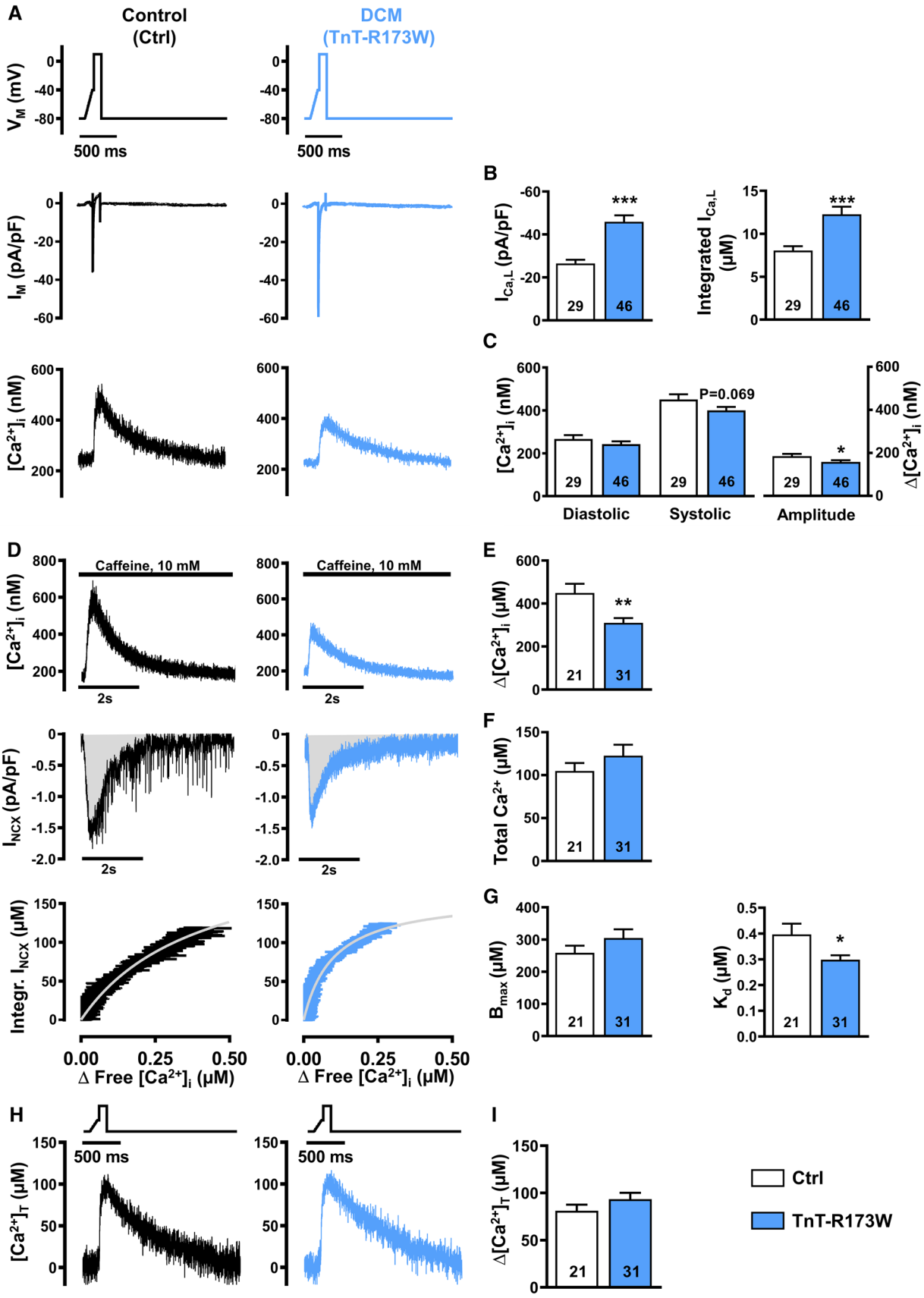
A
Control (Ctrl)
DCM (TnT-R173W)
V_M (mV)
0
-40
-80
500 ms
I_M (pA/pF)
0
-20
-40
-60
$[Ca^{2+}]_i$ (nM)
600
400
200
B
$I_{Ca,L}$ (pA/pF)
-60
-40
-20
0
***
29
46
Integrated $I_{Ca,L}$ (μM)
15
10
5
0
***
29
46
C
$[Ca^{2+}]_i$ (nM)
600
400
200
0
P=0.069
*
29
46
29
46
29
46
Diastolic
Systolic
Amplitude
$\Delta[Ca^{2+}]_i$ (nM)
D
Caffeine, 10 mM
$[Ca^{2+}]_i$ (nM)
800
600
400
200
2s
I_{NCX} (pA/pF)
0
-0.5
-1.0
-1.5
-2.0
Integr. I_{NCX} (μM)
150
100
50
0
0.00
0.25
0.50
Δ Free $[Ca^{2+}]_i$ (μM)
E
$\Delta[Ca^{2+}]_i$ (μM)
600
400
200
0
**
21
31
F
Total Ca^{2+} (μM)
150
100
50
0
21
31
G
B_{max} (μM)
400
300
200
100
0
21
31
K_d (μM)
0.5
0.4
0.3
0.2
0.1
0.0
*
21
31
H
500 ms
$[Ca^{2+}]_T$ (μM)
150
100
50
0
I
$\Delta[Ca^{2+}]_T$ (μM)
150
100
50
0
21
31
Ctrl
TnT-R173W

◂**Fig. 3** $I_{Ca,L}$ and Ca^{2+} transient (upper), sarcoplasmic reticulum Ca^{2+} load and intracellular Ca^{2+} buffering (middle) and total cytosolic Ca^{2+} concentration during $I_{Ca,L}$ triggering (lower) in control (Ctrl) and DCM-TnT-R173W induced pluripotent stem cell-derived cardiomyocytes (iPSC-CM). **A** Voltage-clamp protocol (upper), representative simultaneous recordings of $I_{Ca,L}$ (middle) and corresponding $I_{Ca,L}$-triggered Ca^{2+} transients (CaT, lower) in Ctrl (left) and TnT-R173W (right) iPSC-CM. **B** Peak $I_{Ca,L}$ amplitude (left) and integrated $I_{Ca,L}$ (right). **C** Diastolic and systolic $[Ca^{2+}]_i$ (left) and Ca^{2+} transient amplitude (right). **D** Representative recordings of caffeine-induced Ca^{2+} transient, i.e. free cytosolic Ca^{2+} concentration (upper) with associated depolarising inward current (I_{NCX}, middle) in Ctrl (left) and TnT-R173W (right) iPSC-CM. Integrated I_{NCX} as an index for total cytosolic Ca^{2+} concentration was plotted against corresponding cytosolic free Ca^{2+} concentration (lower). Buffer curves depicting the relationship between cytosolic free and total Ca^{2+} were fitted with hyperbolic functions. **E**, **F** Sarcoplasmic reticulum Ca^{2+}, quantified with caffeine-induced Ca^{2+} transient amplitude (**E**), or area under the curve (Integral) of the corresponding inward current (I_{NCX}) (**F**). **G** Maximum buffer capacity (B_{max}, left) and dissociation constant (K_d, right), determined from buffer curves. **H** Representative total cytosolic Ca^{2+} concentration during $I_{Ca,L}$-triggered Ca^{2+} transients in Ctrl (left) and TnT-R173W (right) iPSC-CM. **I** Total cytosolic Ca^{2+} amplitude. n = number of iPSC-CM from 3 to 5 batches. Data are mean ± SEM. $^*P<0.05$, $^{**}P<0.01$ and $^{***}P<0.001$ vs. Ctrl using Student's t test (**B**, **C**, **E**–**G** left, **I**) and the Mann–Whitney U test (**G** right)

To quantify intracellular Ca^{2+} buffering, the integral of the caffeine-induced NCX current was plotted against free $[Ca^{2+}]$, as determined during the decay of the caffeine-induced Ca^{2+} transient [59, 66]. The data were fitted with a Michaelis–Menten buffer curve (Fig. 3D lower panel):

$$\left[Ca^{2+}\right]_{total} = \frac{B_{max}\left[Ca^{2+}\right]_i}{K_d + \left[Ca^{2+}\right]_i}.$$

The maximum buffer capacity B_{max} was comparable between DCM-TnT-R173W and Ctrl, pointing to a similar amount of cytosolic Ca^{2+}-binding sites. In contrast, the dissociation constant K_d, which represents the $[Ca^{2+}]_i$ at which buffers are half saturated, was significantly lower in DCM-TnT-R173W, compared to Ctrl (Fig. 3G). A lower K_d suggests increased affinity of cytosolic Ca^{2+} buffers, thereby resulting in increased Ca^{2+} buffering in DCM-TnT-R173W.

Based on the estimated values of B_{max} and K_d, Ca^{2+}-buffer curves were calculated for each individual experiment (Supplementary Fig. 5A), allowing estimation of the time course of changes of total cytosolic Ca^{2+} during $I_{Ca,L}$-triggered Ca^{2+} transient (Fig. 3H). In contrast to the lower free cytosolic Ca^{2+} transient amplitude (Fig. 3C right panel), the amplitude of total Ca^{2+} release in DCM-TnT-R173W was comparable to Ctrl (Fig. 3I) suggesting that apparent alterations in systolic Ca^{2+} transients are mainly due to increased Ca^{2+} buffering.

Slower decay of free systolic Ca^{2+} transient in TnT-R173W iPSC-CM is due to increased Ca^{2+} buffering

We further assessed whether the measured changes of cytosolic Ca^{2+} buffering can account quantitatively for the observed slowing of the cytosolic free Ca^{2+} transient [10]. Therefore, we plotted the rate of decay of free Ca^{2+} ($-d[Ca^{2+}]_i/dt$) as a function of the free cytosolic Ca^{2+} level (Fig. 4A) and, in accordance with slower decay of the cytosolic Ca^{2+} transient, we found the gradient of this relationship to be smaller in DCM-TnT-R173W (Fig. 4B). In contrast, Fig. 4C shows the rate of decay of total Ca^{2+} ($-d[Ca^{2+}]_{total}/dt$) plotted against the free $[Ca^{2+}]_i$ with unaltered slope in DCM-TnT-R173W. The unaltered slope shows that the slowed decay of the systolic free Ca^{2+} transient in DCM-TnT-R173W (Fig. 2B) can be attributed quantitatively to increased Ca^{2+} buffering.

To estimate the contribution of NCX to cytosolic Ca^{2+} removal, we plotted the rate of decay of total Ca^{2+} during caffeine-induced Ca^{2+} transient against the corresponding free cytosolic Ca^{2+} level. The resulting slope was comparable between both groups suggesting unaltered activity of NCX (Fig. 4D). In accordance, the slope of the line relating I_{NCX} to $[Ca^{2+}]_i$ during decay of caffeine-induced Ca^{2+} transient (Supplementary Fig. 9A, B) showed no difference between groups, confirming unaltered Ca^{2+}-dependence of NCX function. Since $[Ca^{2+}]_i$ dependence of decay rate of total Ca^{2+} ($d[Ca^{2+}]_{total}/dt$) was unaltered during systolic and caffeine-induced Ca^{2+} transients, it can be concluded that $[Ca^{2+}]_i$ dependence of SERCA activity is unaltered in DCM-TnT-R173W, which has been estimated based on the difference between the two respective slopes (Fig. 4E).

Pharmacological increase in myofilament Ca^{2+} affinity reproduces the Ca^{2+} handling phenotype observed in DCM-R173W iPSC-CM

Since TnC is the major cytosolic Ca^{2+} buffer [59], the DCM-TnT-R173W mutation likely results in increased Ca^{2+} affinity of TnC, leading to increased Ca^{2+} buffering and altered Ca^{2+} homeostasis.

To investigate whether increased Ca^{2+} affinity of myofilaments may contribute to Ca^{2+} handling abnormalities observed in DCM-TnT-R173W iPSC-CM, Ctrl iPSC-CM were treated with the Ca^{2+} sensitiser EMD57033 (5 µM, 5 min pre-treatment, Figs. 5, 6) [1]. EMD57033 treatment had no effect on $I_{Ca,L}$ (Fig. 5B). This is in stark contrast to the greater $I_{Ca,L}$ in DCM-TnT-R173W iPSC-CM, an effect which, therefore, appears to be independent of increased Ca^{2+} buffering. Ca^{2+} transient amplitude was, however, smaller in EMD57033-treated iPSC-CM, compared to Ctrl (Fig. 5C right panel).

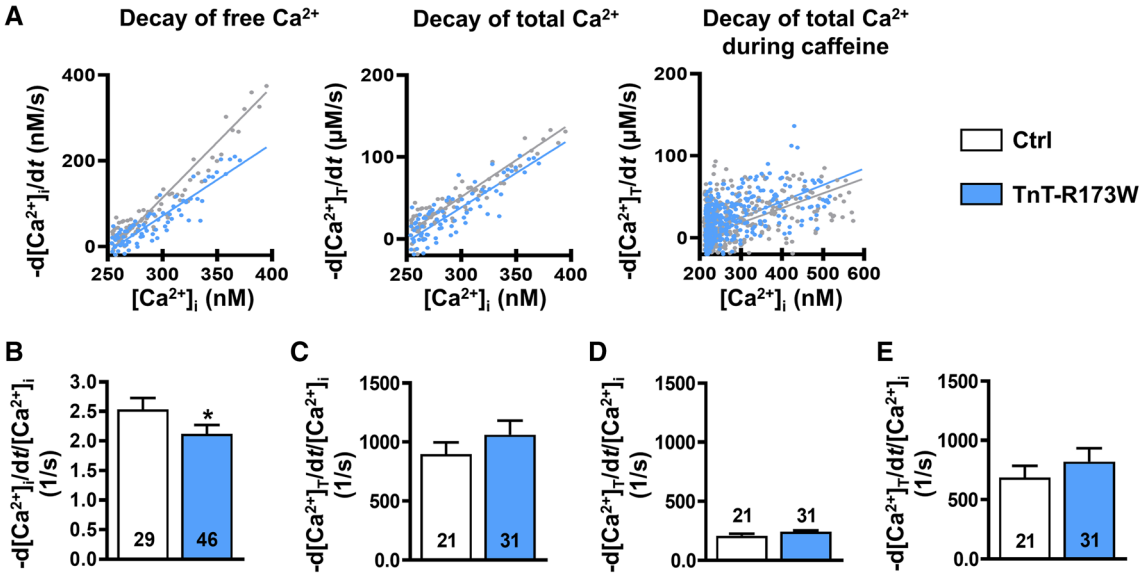

Fig. 4 Quantification of decay of free and total Ca^{2+} transient of control (Ctrl) and DCM-TnT-R173W induced pluripotent stem cell-derived cardiomyocytes (iPSC-CM). **A** Representative rate of decay of free Ca^{2+} ($-d[Ca^{2+}]_i/dt$) plotted against free $[Ca^{2+}]_i$ (left), representative rate of decay of total Ca^{2+} ($-d[Ca^{2+}]_{total}/dt$) plotted against free $[Ca^{2+}]_i$ (middle) and representative rate of decay of total Ca^{2+} during caffeine-induced Ca^{2+} transient plotted against the corresponding free $[Ca^{2+}]_i$ (right) in Ctrl and TnT-R173W iPSC-CM. Slopes are shown as a linear function. **B** Slope of $-d[Ca^{2+}]_i/dt$ plotted against $[Ca^{2+}]_i$. **C** Slope of $-d[Ca^{2+}]_{total}/dt$ plotted against $[Ca^{2+}]_i$. **D** Slope of $-d[Ca^{2+}]_{total}/dt$ during caffeine plotted against the corresponding $[Ca^{2+}]_i$. **E** Difference between C and D indicating unaltered $[Ca^{2+}]_I$ dependence of SERCA-mediated Ca^{2+} removal. n = number of iPSC-CM from 3 to 5 batches. Data are mean ± SEM $^*P < 0.05$ vs. Ctrl using Mann–Whitney U test (**B**, **C**, **E**) and Student's t test (**D**)

EMD57033 treatment did not affect SR Ca^{2+} load, as quantified by the integration of the caffeine-induced I_{NCX} (Fig. 5D middle panel, F). In contrast, amplitude of the caffeine-induced Ca^{2+} transient was smaller in EMD57033-treated iPSC-CM, compared to untreated (Fig. 5E), indicating less free $[Ca^{2+}]_i$ during Ca^{2+} release from the SR. Quantification of buffer properties revealed unaltered total buffer capacity, B_{max}, but a lower dissociation constant, K_d, in EMD57033-treated iPSC-CM (Fig. 5G). These data phenocopy the Ca^{2+} handling properties observed in DCM-TnT-R173W iPSC-CM and confirm the effective increase in cytosolic Ca^{2+} buffering in myocytes treated with EMD57033.

The smaller Ca^{2+} transient amplitude in myocytes treated with EMD57033 is unlikely to be caused by the lower total amount of Ca^{2+} released from the SR because the amplitude of the total Ca^{2+} transient calculated based on Ca^{2+} buffer curves (Supplementary Fig. 5C) was unaltered (Fig. 5H, I). Rather, it is more likely due to stronger binding of Ca^{2+} to myofilaments sensitised by EMD57033. The latter also hampers diastolic Ca^{2+} removal from the cytosol since Ca^{2+} must first dissociate from buffers before it can interact with Ca^{2+} removal mechanisms of the SR and the sarcolemma, respectively. Accordingly, decay of cytosolic free Ca^{2+} during $I_{Ca,L}$-triggered SR Ca^{2+} release was slower in EMD57033-treated iPSC-CM (Fig. 6B). In contrast, $[Ca^{2+}]_i$ dependence of the decay rate of total Ca^{2+} during $I_{Ca,L}$-triggered and caffeine-induced SR Ca^{2+} release was unaltered in EMD57033-treated cells pointing to unchanged SERCA and NCX $[Ca^{2+}]_i$ dependence (Fig. 6C–E).

To demonstrate that increased Ca^{2+} buffering is sufficient to increase alternans susceptibility, field stimulation experiments were performed in EMD57033-treated iPSC-CM (Fig. 7). Similar to DCM-TnT-R173W, Ca^{2+} transient upstroke was slower (Supplementary Fig. 4B) and time constant of decay was greater in EMD57033-treated iPSC-CM, compared to Ctrl (Fig. 7B). Furthermore, EMD57033-treated iPSC-CM demonstrated higher susceptibility for Ca^{2+} alternans, as shown by the Kaplan–Meier curve (Fig. 7D), and a lower threshold frequency for Ca^{2+} transient alternans, compared to Ctrl (Fig. 7C).

Blebbistatin reduces alternans susceptibility in DCM-TnT-R173W iPSC-CM

Blebbistatin is an inhibitor of myosin ATPase and has been suggested to reduce Ca^{2+} affinity of myofilaments [1]. To test whether the proarrhythmic phenotype of DCM-TnT-R173W iPSC-CM may be rescued by normalisation of myofilament Ca^{2+} affinity, Ca^{2+} transients were recorded in electrically field stimulated DCM-TnT-R173W iPSC-CM treated with blebbistatin (10 µM, 20 min pre-treatment, Fig. 8). As shown in Fig. 8B, blebbistatin treatment normalised Ca^{2+} transient

time constant of decay. In addition, blebbistatin reduced susceptibility to Ca^{2+} transient alternans in DCM-TnT-R173W iPSC-CM and increased the threshold frequency at which Ca^{2+} transient alternans occurred (Fig. 8C, D).

Discussion

In the current study, iPSC-CM with the DCM-TnT-R173W mutation were used to assess Ca^{2+} handling abnormalities and examine the arrhythmogenic propensity of patients with DCM. Single-cell patch-clamp experiments revealed increased intracellular Ca^{2+} buffering in DCM-TnT-R173W iPSC-CM. In addition, it could be demonstrated that these alterations in cytosolic Ca^{2+} handling contribute to AP and Ca^{2+} transient alternans as a potential underlying substrate for increased arrhythmogenesis in DCM patients harbouring the DCM-TnT-R173W mutation. Of note, treatment with blebbistatin, a myosin ATPase inhibitor causing decreased myofilament Ca^{2+} sensitivity [1], reduced the occurrence of Ca^{2+} alternans in DCM-TnT-R173W iPSC-CM. Our findings suggest that modulation of myofilament Ca^{2+} sensitivity may represent a potential anti-arrhythmic concept in DCM patients, in particular in those harbouring mutations in TnT.

Cardiac arrhythmia mechanisms in DCM patients

DCM patients are more prone to cardiac arrhythmia development, with the main reasons for mortality being end-organ dysfunction due to heart failure or arrhythmia-related death [65]. Premature ventricular contractions and non-sustained ventricular tachycardia are common in DCM and are observed in up to 90% and 60% of patients, respectively. Cardiac arrest can occur due to monomorphic or polymorphic ventricular tachycardia, degenerating to ventricular fibrillation [27].

A variety of mechanisms have been proposed to contribute to arrhythmogenesis in patients with DCM, but the primary cause is not well understood [27]. DCM patients often present with multiple patchy areas of replacement fibrosis, which can act as sites for re-entry, one of the most common mechanisms underlying ventricular tachycardia and sudden cardiac death [40, 55]. Other hypotheses focus on abnormal wall stretch, causing alterations in ventricular refractoriness and predisposing the patient to abnormal automaticity and triggered activity [6].

Given the broad spectrum of genetic and non-genetic contributors to DCM pathophysiology, the identification of a common pathomechanism underlying arrhythmogenesis in all DCM patients is almost impossible. Valvular heart disease, excessive alcohol consumption, hypertension and infectious diseases, for example, are accepted etiological factors associated with disease-specific remodelling pathways leading to DCM [42]. Nevertheless, in about 40% of patients with DCM, underlying genetic factors are thought to play a role [18]. Most mutations causing DCM are located in genes encoding for cytoskeletal, sarcolemmal and sarcomeric proteins [31, 42]. A "disruption" in the link between these three components and consecutive disturbance of ion-channel function have been proposed as the "final common pathway" in DCM arrhythmogenesis [65].

Many DCM-causing mutations have also been shown to affect multiple aspects of Ca^{2+} homeostasis in cardiac myocytes, including altered binding of Ca^{2+} to myofilaments, as well as disrupted expression of Ca^{2+} handling proteins. It follows, therefore, that abnormal Ca^{2+} handling may also play a potentially key role in DCM-related arrhythmogenesis [30, 64].

Altered cytosolic Ca^{2+} handling in DCM patients

Ca^{2+} is a major mediator of excitation–contraction coupling [4] and specific alterations in cellular Ca^{2+} handling are likely to contribute to impaired contractile function in patients with DCM [31]. Accordingly, decreased amplitude of systolic Ca^{2+} transients appears to be a common finding in all DCM models in which cytosolic Ca^{2+} handling has been investigated [2, 36, 37, 62, 63]. Reduced Ca^{2+} transient amplitude has been suggested to result from reduced SR Ca^{2+} content, which may be due to increased diastolic Ca^{2+} leak from the SR mediated by leaky type 2 ryanodine receptor channels (RyR2) [2]. Reduced SR Ca^{2+} content may also result from slower Ca^{2+} reuptake into the SR due to reduced activity of SERCA [43].

Here, we describe another mechanism which could also contribute to reduced Ca^{2+} transient amplitude in DCM patients. Our experiments suggest that reduced Ca^{2+} transient amplitude in DCM-TnT-R173W cardiomyocytes [63] results from increased Ca^{2+} buffering due to increased binding of Ca^{2+} to myofilaments [14]. This is consistent with previous publications showing that the DCM-TnT-R173W mutation limits binding of protein kinase A to local sarcomere microdomains, thereby attenuating phosphorylation of TnI [9]. The latter might contribute to increasing the Ca^{2+} sensitivity of TnC and increase Ca^{2+}-myofilament binding within the physiologically relevant range (Supplementary Figs. 5B, D).

It is important to note that contractile function is attenuated in DCM-TnT-R173W myocytes and engineered heart muscle constructs (EHM) [9, 39]. A contributing factor might be the reduced interaction of TnT with tropomyosin in the presence of the DCM-TnT-R173W mutation, which is located within one of the two tropomyosin binding regions of TnT [9, 24]. This may affect correct relocation of tropomyosin following Ca^{2+} binding to TnC as well as freeing of the myosin-binding sites on actin, thereby limiting contraction.

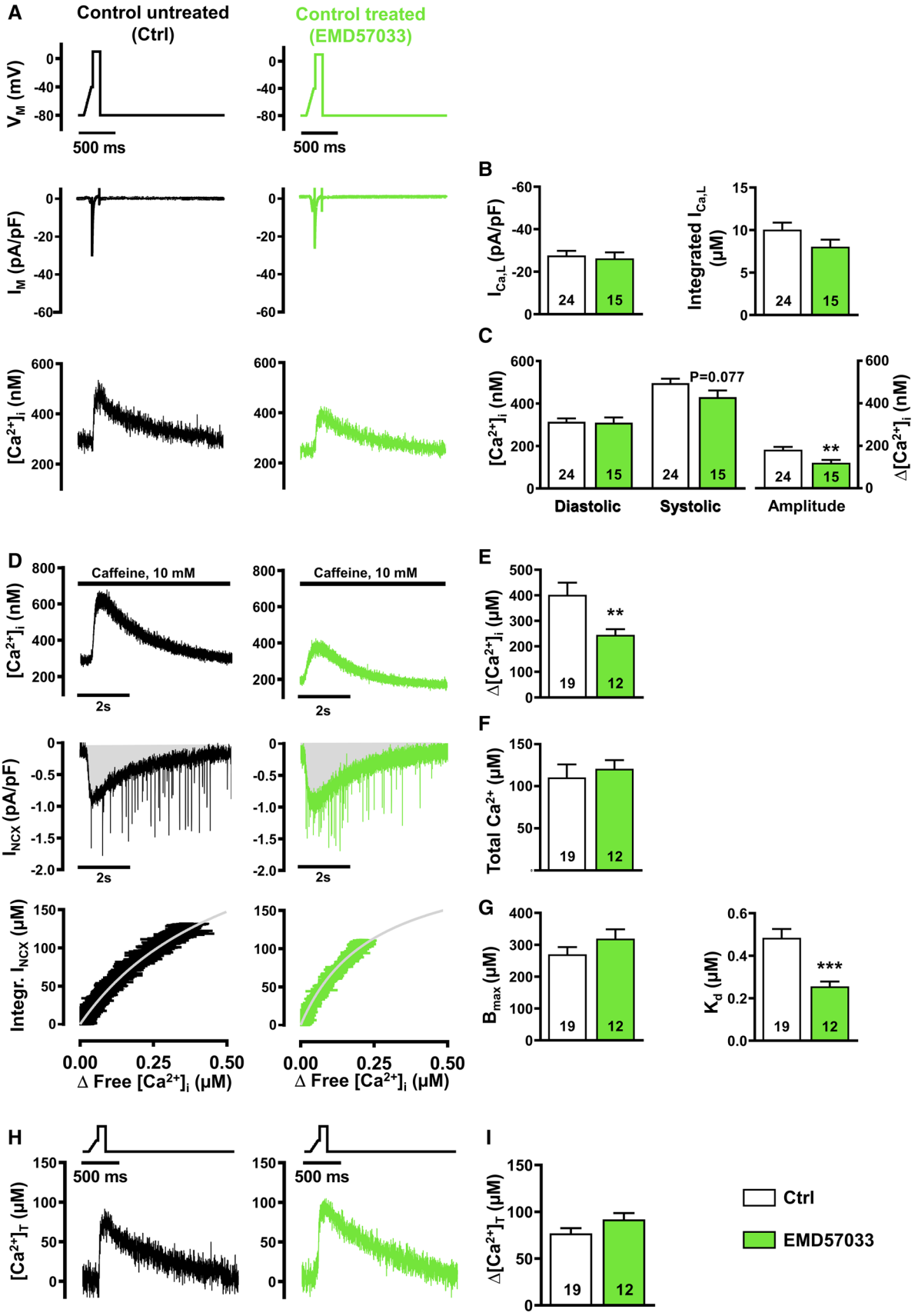
A
Control untreated (Ctrl)
Control treated (EMD57033)
V_M (mV)
0
-40
-80
500 ms
I_M (pA/pF)
0
-20
-40
-60
$[Ca^{2+}]_i$ (nM)
600
400
200
B
$I_{Ca,L}$ (pA/pF)
-60
-40
-20
0
24
15
Integrated $I_{Ca,L}$ (µM)
15
10
5
0
C
$[Ca^{2+}]_i$ (nM)
P=0.077
$\Delta[Ca^{2+}]_i$ (nM)
**
Diastolic
Systolic
Amplitude
D
Caffeine, 10 mM
2s
I_{NCX} (pA/pF)
-0.5
-1.0
-1.5
-2.0
Integr. I_{NCX} (µM)
150
100
50
0
0.00
0.25
0.50
Δ Free $[Ca^{2+}]_i$ (µM)
E
$\Delta[Ca^{2+}]_i$ (µM)
19
12
F
Total Ca^{2+} (µM)
G
B_{max} (µM)
K_d (µM)
***
H
$[Ca^{2+}]_T$ (µM)
I
$\Delta[Ca^{2+}]_T$ (µM)
Ctrl
EMD57033

◂**Fig. 5** $I_{Ca,L}$ and Ca^{2+} transient (upper), sarcoplasmic reticulum Ca^{2+} load and intracellular Ca^{2+} buffering (middle) and total cytosolic Ca^{2+} concentrations during $I_{Ca,L}$ triggering (lower) in control (Ctrl) induced pluripotent stem cell-derived cardiomyocytes (iPSC-CM) pre-treated with EMD57033 (5 µM). **A** Voltage-clamp protocol (upper), representative simultaneous recordings of $I_{Ca,L}$ (middle) and corresponding $I_{Ca,L}$-triggered Ca^{2+} transients (CaT, lower) in untreated Ctrl iPSC-CM (left) and Ctrl iPSC-CM pre-treated with EMD57033 (right). **B** Peak $I_{Ca,L}$ amplitude (left) and integrated $I_{Ca,L}$ (right). **C** Diastolic and systolic $[Ca^{2+}]_i$ (left) and Ca^{2+} transient amplitude (right). **D** Representative recordings of caffeine-induced Ca^{2+} transient i.e. free cytosolic Ca^{2+} concentration (upper) with associated depolarising inward current (I_{NCX}, middle) in untreated Ctrl iPSC-CM (left) and Ctrl iPSC-CM pre-treated with EMD57033 (right). Integrated I_{NCX} as an index for total cytosolic Ca^{2+} concentration was plotted against corresponding cytosolic free Ca^{2+} concentration (lower). Buffer curves depicting the relationship between cytosolic free and total Ca^{2+} were fitted with hyperbolic functions. **E**, **F** Sarcoplasmic reticulum Ca^{2+}, quantified with caffeine-induced Ca^{2+} transient amplitude (**E**), or area under the curve (Integral) of the corresponding inward current (I_{NCX}) (**F**). **G** Maximum buffer capacity (B_{max}, left) and dissociation constant (K_d, right), determined from buffer curves. **H** Representative total cytosolic Ca^{2+} concentration during $I_{Ca,L}$-triggered Ca^{2+} transients in untreated Ctrl iPSC-CM (left) and Ctrl iPSC-CM pre-treated with EMD57033 (right). **I** Total cytosolic Ca^{2+} amplitude. n = number of iPSC-CM from three batches. Data are mean ± SEM. $^{**}P < 0.01$ and $^{***}P < 0.001$ vs. Ctrl using Student's t test (**B**, **C** left, **F**, **G**, **I**) and the Mann–Whitney U test (**C** right, **E**)

A similar discrepancy has been shown in skinned muscle fibres in response to caffeine, which sensitises the force response to lower Ca^{2+} concentrations without affecting Ca^{2+} binding to TnC [53]. Taken together it is important to consider alterations in the "apparent" Ca^{2+} affinity of contractile proteins determined by analysis of contractile function in response to variations of $[Ca^{2+}]_i$ separately from alterations in the Ca^{2+} binding affinity of myofilaments. The latter represent the major Ca^{2+} buffers in cardiac myocytes and alterations in binding affinity are thought to have relevant impact on cellular Ca^{2+} homeostasis [59].

Increased susceptibility to arrhythmogenic AP and Ca^{2+} transient alternans in DCM patients

Increased Ca^{2+} buffering has a major impact on Ca^{2+} handling and arrhythmogenesis [14]; Ca^{2+} influences cellular electrophysiology via the modulation of Ca^{2+}-dependent ion channels and transporters in the sarcolemma, such as the L-type Ca^{2+} channel and NCX. It, therefore, follows that altered Ca^{2+} handling may also contribute to arrhythmogenesis in patients with DCM. Surprisingly little is known about the role abnormal Ca^{2+} handling plays in arrhythmogenesis in patients with DCM. Previous publications have shown that increased incidence of spontaneous Ca^{2+} release events from the SR during diastole may contribute to arrhythmogenesis, particularly in patients with Duchenne Muscular Dystrophy (DMD)-associated cardiomyopathy [2]. The released Ca^{2+} is extruded from the myocyte by NCX, which brings 3 Na^+ ions per extruded Ca^{2+} ion into the cell, giving rise to a depolarising inward current. If this current is large enough, it will trigger a new action potential and ectopic activity, with the potential to initiate cardiac arrhythmias [20, 70, 71].

Here, we demonstrate for the first time that cardiomyocytes from patients harbouring a DCM-causing mutation are prone to developing arrhythmogenic AP and Ca^{2+} transient alternans. The maximum slope of the AP restitution curves did not exceed one (Fig. 1B), which points towards Ca^{2+}-driven alternans as opposed to alternans based on AP which requires a steeper restitution slope [15, 73]. In addition, the alterations in Ca^{2+} handling properties seen in DCM-TnT-R173W iPSC-CM could be reproduced in control iPSC-CM treated with the Ca^{2+} sensitiser EMD57033. This highlights increased Ca^{2+} buffering as a major contributor to impaired Ca^{2+} handling and increased susceptibility to arrhythmogenic alternans in DCM-TnT-R173W iPSC-CM.

Ca^{2+} alternans is enhanced by factors which increase SR Ca^{2+} release and reduce Ca^{2+} sequestration from the cytosol [73]. Increased Ca^{2+} buffering has previously been shown to reduce Ca^{2+} reuptake into the SR [10, 59]. In the present study, Ca^{2+} transient decay was slower in DCM-TnT-R173W iPSC-CM. We suggest that this is predominantly due to slowed SERCA and NCX-mediated Ca^{2+} removal from the cytosol secondary to increased Ca^{2+} buffering by myofilaments. Since NCX-mediated Ca^{2+} removal is electrogenic, the slower Ca^{2+} transient decay, it generates a depolarising inward current resulting in slower repolarisation of the membrane potential during diastole. Indeed, further analysis of diastolic potentials during optical AP recordings revealed a significantly increased diastolic potential preceding every even ("pathological") beat compared with every odd ("physiological") AP. This is consistent with incomplete diastolic extrusion of intracellular Ca^{2+} in DCM-TnT-R173W iPSC-CM and persistence of NCX current (Supplementary Fig. 3F, G). The higher diastolic membrane potential prevents recovery from inactivation of voltage-gated ion channels thereby leading to impaired AP upstroke and/or duration. Since the abnormal AP appears not sufficient for triggering full SR Ca^{2+} release, cytosolic Ca^{2+} is reduced to its initial state without remaining NCX current, thereby allowing full repolarization of the membrane potential and the alternans cycle starts all over again [73].

AP and Ca^{2+} transient alternans may lead to spatial electrical heterogeneity, providing a substrate for arrhythmogenic activity [16, 46]. Interestingly, a similar arrhythmogenic mechanism has been proposed by Baudenbacher et al. in mouse models harbouring TnT mutations causing hypertrophic cardiomyopathy [1]. The authors demonstrated that the risk of developing ventricular tachycardia was directly proportional to the degree of Ca^{2+} sensitisation caused by

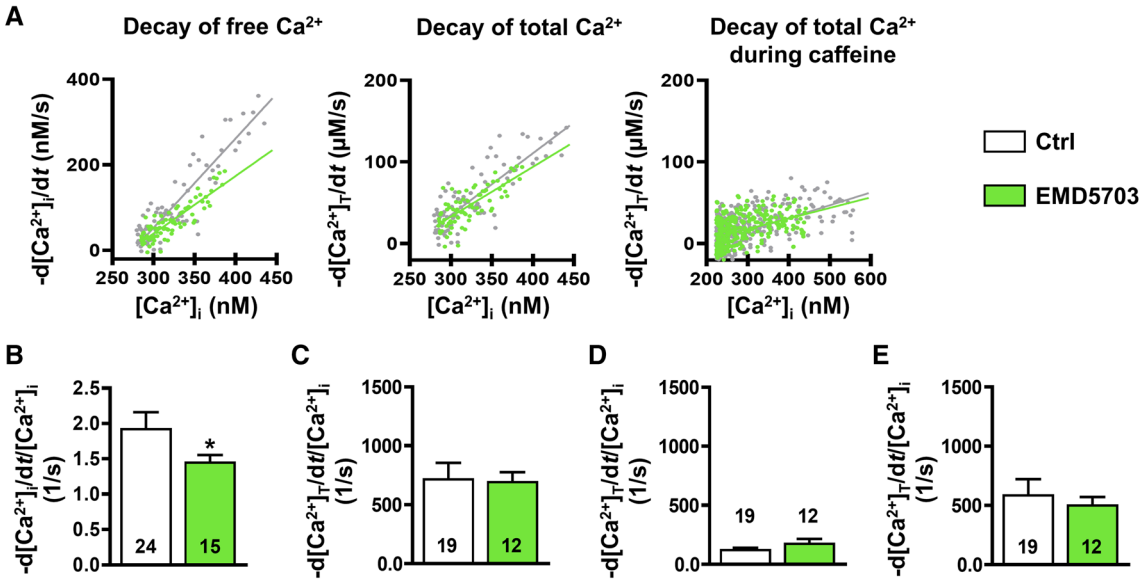

Fig. 6 Quantification of decay of free and total Ca^{2+} transient in control (Ctrl) induced pluripotent stem cell-derived cardiomyocytes (iPSC-CM) pre-treated with EMD57033 (5 µM). **A** Representative rate of decay of free Ca^{2+} ($-d[Ca^{2+}]_i/dt$) plotted against free $[Ca^{2+}]_i$ (left), representative rate of decay of total Ca^{2+} ($-d[Ca^{2+}]_{total}/dt$) plotted against free $[Ca^{2+}]_i$ (middle) and representative rate of decay of total Ca^{2+} during caffeine-induced Ca^{2+} transient plotted against the corresponding free $[Ca^{2+}]_i$ (right) in Ctrl iPSC-CM with and without EMD57033 treatment. Slopes are shown as a linear function. **B** Slope of $-d[Ca^{2+}]_i/dt$ plotted against $[Ca^{2+}]_i$. **C** Slope of $-d[Ca^{2+}]_{total}/dt$ plotted against $[Ca^{2+}]_I$. **D** Slope of $-d[Ca^{2+}]_{total}/dt$ during caffeine plotted against the corresponding $[Ca^{2+}]_i$. **E** Difference between C and D indicating unaltered $[Ca^{2+}]_I$ dependence of SERCA-mediated Ca^{2+} removal. n = number of iPSC-CM from three batches. Data are mean ± SEM. $^*P < 0.05$ vs. Ctrl using Mann–Whitney U test (**B**–**E**)

the mutation. Furthermore, in vitro studies demonstrate that HCM-causing mutations sensitising myofilaments to Ca^{2+} are associated with high risk of sudden cardiac death [17, 20, 26, 57, 72]. There is also evidence for increased myofilament Ca^{2+} sensitivity in ventricular myocytes after myocardial infarction and also from patients with heart failure. Both diseases are associated with a high incidence of ventricular tachycardia and sudden cardiac death [68, 69, 74]. Our data show, for the first time, that increased Ca^{2+} buffering and increased susceptibility to AP and Ca^{2+} alternans also occur in myocytes from DCM-TnT-R173W patients. The extent to which our findings are valid in other subsets of DCM patients requires further investigation.

Potential limitations

In the present study, we used iPSC-CM from DCM patients harbouring the TnT-R173 mutation. iPSC-CM represent myocytes at an immature developmental stage. iPSC-CM exhibit poor co-localisation between $I_{Ca,L}$ channels and RYR2 [54], resulting in more internal, non-coupled RyRs being activated by the subsequent rise in $[Ca^{2+}]_i$ as opposed to direct activation by $I_{Ca,L}$ channels [32, 78]. Nevertheless, iPSC-CM resemble adult ventricular cardiomyocytes in many aspects of cellular electrophysiology, Ca^{2+} handling and contractile function [12, 23]. In addition, human iPSC-CM present a readily available human model of cardiac myocytes which can be generated on demand in large quantities [7, 11, 13], making them a promising model to investigate electrophysiological abnormalities in patients with inherited cardiac arrhythmias [22, 44, 77].

Our data show significant upregulation of $I_{Ca,L}$ in DCM-TnT-R173W iPSC-CM. In contrast, SR Ca^{2+} content was unchanged in DCM-TnT-R173W iPSC-CM (Fig. 3F). Since the latter is mainly determined by the Ca^{2+} influx-efflux balance, this points to increased diastolic Ca^{2+} efflux [47, 67]. Accordingly, the amount of Ca^{2+} removed by NCX correlated with the Ca^{2+} influx mediated by $I_{Ca,L}$ (Supplementary Fig. 9D, E). In addition, Ca^{2+} removal by forward mode NCX was increased in DCM-TnT-R173W iPSC-CM to compensate for the higher Ca^{2+} influx through upregulated $I_{Ca,L}$. The mechanisms underlying increased $I_{Ca,L}$ are beyond the scope of the present study. Nevertheless, unaltered mRNA expression of the underlying Ca^{2+} channel subunit, Cav1.2, renders intrinsic differences of its expression levels between DCM-TnT-R173W and Ctrl iPSC-CM unlikely (Supplementary Fig. 6). Further analysis of the biphasic $I_{Ca,L}$ inactivation revealed unaltered time course of fast $I_{Ca,L}$ decay (τ_{fast}, Supplementary Fig. 7A left panel), which is thought to be mainly due to Ca^{2+} dependent inactivation of $I_{Ca,L}$ [3]. We, therefore, conclude that increased $I_{Ca,L}$ in DCM-TnT-R173W is unlikely due to reduced Ca^{2+}-dependent inhibition of

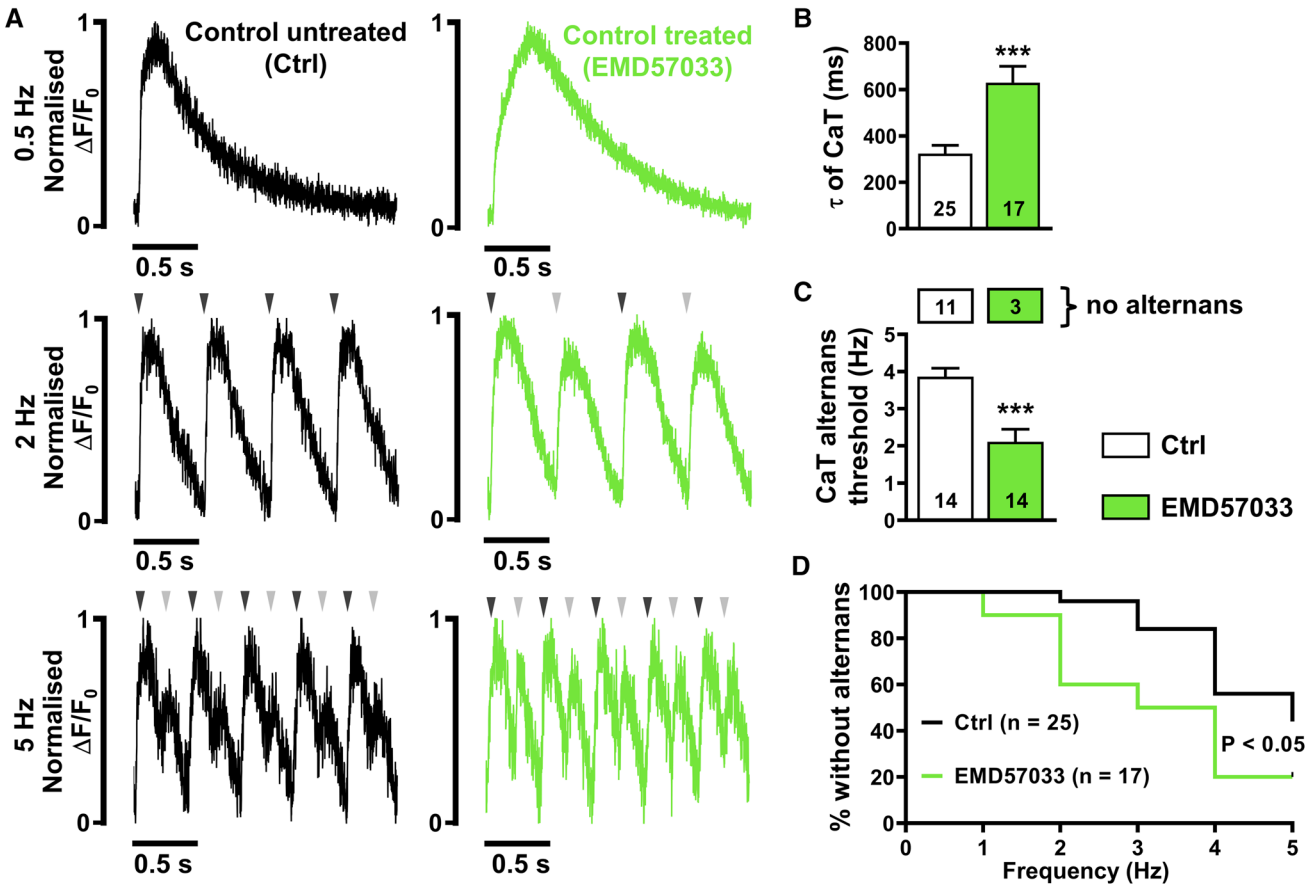

Fig. 7 Incidence of Ca^{2+} alternans in control (Ctrl) induced pluripotent stem cell-derived cardiomyocytes (iPSC-CM) pre-treated with EMD57033 (5 µM). **A** Normalised representative traces of Ca^{2+} transients (CaT) at 0.5 Hz (upper), 2 Hz (middle) and 5 Hz (lower) in untreated Ctrl (left) and in Ctrl iPSC-CM pre-treated with EMD57033 (right). Arrowheads indicate electrical stimulation and illustrate when beat-to-beat alterations are present. **B** Ca^{2+} transient time constant of decay (τ). **C** Alternans threshold frequency. Number of myocytes without alternans is shown in boxes above. **D** Kaplan–Meier plot showing the percentage of cells without alternans in relation to the respective pacing. n = number of iPSC-CM from 2 to 5 batches. Data are mean ± SEM. $^*P < 0.05$ and $^{***}P < 0.001$ vs. Ctrl using the Mann–Whitney U test (**B**, **C**), and the Gehan–Breslow–Wilcoxon test (**D**)

$I_{Ca,L}$ in response to reduced free cytosolic Ca^{2+} levels. In accordance, increased cytosolic buffering due to EMD57033 leads to a similar decrease in Ca^{2+} transient amplitude but had no effect on $I_{Ca,L}$. $I_{Ca,L}$ is regulated by various post-transcriptional and post-translational mechanisms including miRNA-dependent inhibition, phosphorylation and expression of accessory units [19, 56]. Future studies are necessary to investigate whether these mechanisms contribute to $I_{Ca,L}$ alterations in DCM patients in general, but also those harbouring the TnT-R173W mutation.

Despite greater $I_{Ca,L}$, the triggered Ca^{2+} transient amplitude was smaller in DCM-TnT-R173W compared to Ctrl. Based on our experiments, we conclude that this is largely due to increased cytosolic Ca^{2+} buffering. In accordance, the total amount of Ca^{2+} released from the SR during $I_{Ca,L}$-triggered Ca^{2+} transients was unaltered in DCM-TnT-R173W (Fig. 3H). Nevertheless, coupling efficiency between Ca^{2+} influx and total Ca^{2+} release was reduced in DCM-TnT-R173W (Supplementary Fig. 8A). Therefore, impaired interaction between L-type Ca^{2+} channel and RyR2 may additionally contribute to reduced free $I_{Ca,L}$-triggered Ca^{2+} transient amplitude.

To quantify cytosolic Ca^{2+} buffering, we employed a method that allows investigation of Ca^{2+} homeostasis in intact cardiomyocytes [66]. Intracellular Ca^{2+} has been quantified by the fluorescent Ca^{2+} indicator Fluo-3, which represents an intracellular Ca^{2+} buffer itself. We assume that the contribution of Fluo-3 to intracellular Ca^{2+} buffering is comparable between experimental groups and does not contribute to the differences observed in the present study. Based on the dissociation constant ($K_d = 0.864$ µM) and an estimated buffer concentration (b_{max}) of 100 µM, the contribution of Fluo-3 to the calculated buffer curves is illustrated in Supplementary Fig. 5. In addition, the employed techniques do only allow indirect conclusions on altered Ca^{2+}-binding to the troponin complex. Direct quantification

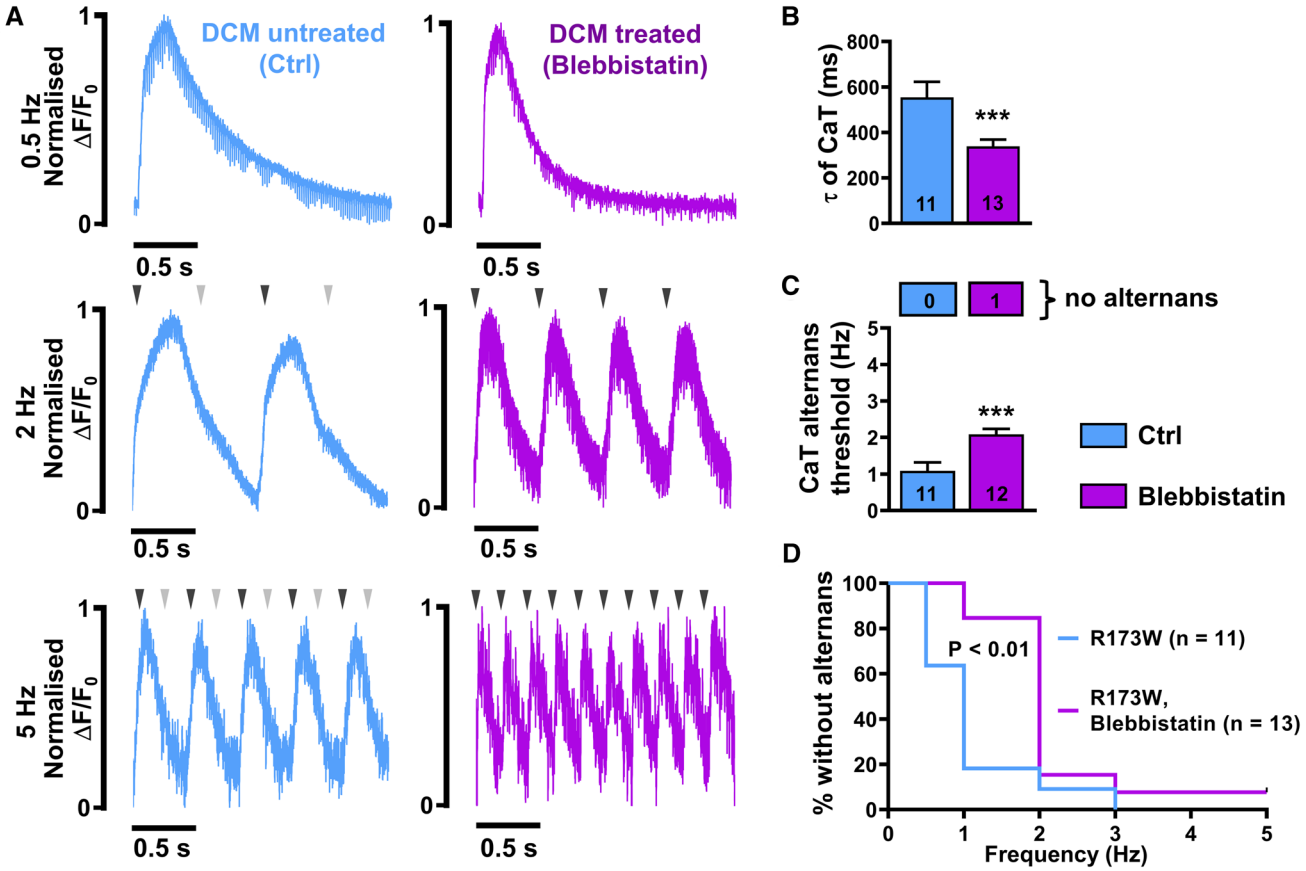

Fig. 8 Incidence of Ca^{2+} alternans in DCM-TnT-R173W induced pluripotent stem cell-derived cardiomyocytes (iPSC-CM) pre-treated with blebbistatin (10 µM). **A** Normalised representative traces of Ca^{2+} transients (CaT) at 0.5 Hz (upper), 2 Hz (middle) and 5 Hz (lower) in untreated TnT-R173W iPSC-CM (left) and in TnT-R173W iPSC-CM pre-treated with blebbistatin (right). Arrowheads indicate electrical stimulation and illustrate when beat-to-beat alterations are present. **B** Ca^{2+} transient time constant of decay (τ). **C** Alternans threshold frequency. Number of myocytes without alternans is shown in boxes above. **D** Kaplan–Meier plot showing the percentage of cells without alternans in relation to the respective pacing. n = number of iPSC-CM from two batches. Data are mean ± SEM. $^{**}P < 0.01$ vs. Ctrl using the Mann–Whitney U test (**B**, **C**), and the Gehan–Breslow–Wilcoxon test (**D**)

of Ca^{2+} binding to troponin C will require further biochemical analysis that are beyond the scope of the present study [61].

In the present study, we investigated Ca^{2+} handling abnormalities in iPSC-CM carrying a specific mutation in cardiac TnT that has been associated with the occurrence of DCM. Given the multifactorial aetiology of DCM, it is unclear whether reduced Ca^{2+} uptake by SERCA, secondary to increased Ca^{2+} buffering by myofilaments may represent a "final common pathway" underlying arrhythmogenesis in DCM patients [65]. Nevertheless, early studies in ventricular biopsies from DCM patients also revealed a decreased rate of diastolic Ca^{2+} reuptake into the SR [36]. Furthermore, increased Ca^{2+} sensitivity of contraction has also been found in patients and a dog model of pacing induced DCM [45, 75]. The differences in Ca^{2+} sensitivity were abrogated after treatment with the catalytic subunit of PKA, suggesting that, as in DCM caused by TnT-R173W mutations, the increased Ca^{2+} sensitivity of myofilaments may be due to a reduction in PKA-mediated phosphorylation of myofibrillar regulatory proteins.

Outlook

Based on our findings and given the fact that increased myofilament affinity for Ca^{2+} may contribute to arrhythmogenesis in various cardiac diseases, modulation of myofilament Ca^{2+} sensitivity may represent an important novel concept to prevent cardiac arrhythmias [1, 59].

Targeting Ca^{2+} binding of myofilaments is a classical therapeutic concept to improve contractile dysfunction in heart failure patients. Levosimendan and omecamtiv represent traditional drugs aiming to improve contractile force by increasing Ca^{2+} sensitivity and Ca^{2+}-myofilament binding [38, 49]. Nevertheless, it is important to note that levosimendan also increases the incidence of ventricular

arrhythmias in patients with heart failure, likely due to alternans of Ca^{2+} [1, 20].

Blebbistatin is an inhibitor of the myosin ATPase and has been shown to prevent the occurrence of Ca^{2+} alternans in mouse hearts harbouring Ca^{2+}-sensitising TnT mutations in vitro [1]. According to our data, blebbistatin also prevents Ca^{2+} alternans in DCM-TnT-R173W iPSC-CM. Similar to blebbistatin, mavacamten, a small molecule modulator of β-cardiac myosin, which has been recently evaluated in patients with hypertrophic cardiomyopathy, has also been shown to reduce Ca^{2+} affinity of myofilaments [48]. Both blebbistatin and mavacamten may, therefore, represent interesting lead compounds for the development of novel anti-arrhythmic concepts.

Supplementary Information The online version contains supplementary material available at https://doi.org/10.1007/s00395-022-00912-z.

Acknowledgements The authors thank Stefanie Kestel for excellent technical assistance and Maren Dilaj for excellent secretarial help.

Author contributions P.J., F.S., F.E.F. and M.R. performed experiments on cellular electrophysiology and Ca^{2+} handling. N.I. and S.S. performed culture and cardiac differentiation of iPSCs, immunohistochemistry and qRTPCR experiments; H.L provided statistical analysis and expertise; F.E.M analysed data and critically reviewed the manuscript. N.V. designed and supervised the study and wrote the manuscript; A.E. provided critical suggestions, supervision, and wrote the manuscript.

Funding Open Access funding enabled and organized by Projekt DEAL. This work was supported by the Deutsche Forschungsgemeinschaft (DFG) to NV (VO 1568/3-1, VO 1568/4-1, IRTG1816 project 12, SFB1002 project A13 and under Germany's Excellence Strategy—EXC 2067/1-390729940), to AE (SFB1002 Projekt A12), the Deutsche Stiftung für Herzforschung Projekt F/13/20 to AE, DZHK (German Center for Cardiovascular Research, 81X2300189 and 81X4300102) to NV. This work was further supported by scholarships from the Göttingen Promotionskolleg für Medizinstudierende, funded by the Jacob-Henle-Programm and the Else-Kröner-Fresenius-Stiftung to PJ and MR, respectively, and from the German Academic Exchange Service (DAAD) to NI. We are grateful for support from the Clinic for Cardiology and Pneumology at the University Medical Center, Göttingen.

Data availability All available data are incorporated into this article and its online supplementary material.

Code availability Not applicable.

Declarations

Conflict of interest None (all the authors).

Ethical approval All the protocols were approved by the Ethics Committee of the University Medical Center Göttingen (No. 10/9/15 and 15/2/20).

References

1. Baudenbacher F, Schober T, Pinto JR, Sidorov VY, Hilliard F, Solaro RJ, Potter JD, Knollmann BC (2008) Myofilament Ca^{2+} sensitization causes susceptibility to cardiac arrhythmia in mice. J Clin Invest 118:3893–3903. https://doi.org/10.1172/JCI36642
2. Bellinger AM, Reiken S, Carlson C, Mongillo M, Liu X, Rothman L, Matecki S, Lacampagne A, Marks AR (2009) Hypernitrosylated ryanodine receptor/calcium release channels are leaky in dystrophic muscle. Nat Med 15:325–330. https://doi.org/10.1038/nm.1916
3. Bers DM (2001) Excitation-contraction coupling and cardiac contractile force, 2nd edn. Springer Science+Business Media, Dordrecht
4. Bers DM (2002) Cardiac excitation–contraction coupling. Nature 415:198–205. https://doi.org/10.1038/415198a
5. Bollen IAE, Schuldt M, Harakalova M, Vink A, Asselbergs FW, Pinto JR, Krüger M, Kuster DWD, van der Velden J (2017) Genotype-specific pathogenic effects in human dilated cardiomyopathy. J Physiol 595:4677–4693. https://doi.org/10.1113/JP274145
6. Brachmann J, Hilbel T, Grünig E, Benz A, Haass M, Kübler W (1997) Ventricular arrhythmias in dilated cardiomyopathy. Pacing Clin Electrophysiol 20:2714–2718. https://doi.org/10.1111/j.1540-8159.1997.tb06121.x
7. Burridge PW, Matsa E, Shukla P, Lin ZC, Churko JM, Ebert AD, Lan F, Diecke S, Huber B, Mordwinkin NM, Plews JR, Abilez OJ, Cui B, Gold JD, Wu JC (2014) Chemically defined generation of human cardiomyocytes. Nat Methods 11:855–860. https://doi.org/10.1038/nmeth.2999
8. Chen G, Gulbranson DR, Hou Z, Bolin JM, Ruotti V, Probasco MD, Smuga-Otto K, Howden SE, Diol NR, Propson NE, Wagner R, Lee GO, Antosiewicz-Bourget J, Teng JMC, Thomson JA (2011) Chemically defined conditions for human iPSC derivation and culture. Nat Methods 8:424–429. https://doi.org/10.1038/nmeth.1593
9. Dai Y, Amenov A, Ignatyeva N, Koschinski A, Xu H, Soong PL, Tiburcy M, Linke WA, Zaccolo M, Hasenfuss G, Zimmermann W-H, Ebert AD (2020) Troponin destabilization impairs sarcomere-cytoskeleton interactions in iPSC-derived cardiomyocytes from dilated cardiomyopathy patients. Sci Rep 10:209. https://doi.org/10.1038/s41598-019-56597-3
10. Díaz ME, Trafford AW, Eisner DA (2001) The effects of exogenous calcium buffers on the systolic calcium transient in rat ventricular myocytes. Biophys J 80:1915–1925
11. Ebert AD, Diecke S, Chen IY, Wu JC (2015) Reprogramming and transdifferentiation for cardiovascular development and regenerative medicine: where do we stand? EMBO Mol Med 7:1090–1103. https://doi.org/10.15252/emmm.201504395
12. Ebert AD, Joshi AU, Andorf S, Dai Y, Sampathkumar S, Chen H, Li Y, Garg P, Toischer K, Hasenfuss G, Mochly-Rosen D, Wu JC (2019) Proteasome-dependent regulation of distinct

metabolic states during long-term culture of human iPSC-derived cardiomyocytes. Circ Res 125:90–103. https://doi.org/10.1161/CIRCRESAHA.118.313973
13. Ebert AD, Kodo K, Liang P, Wu H, Huber BC, Riegler J, Churko J, Lee J, de Almeida P, Lan F, Diecke S, Burridge PW, Gold JD, Mochly-Rosen D, Wu JC (2014) Characterization of the molecular mechanisms underlying increased ischemic damage in the aldehyde dehydrogenase 2 genetic polymorphism using a human induced pluripotent stem cell model system. Sci Transl Med 6:255ra130. https://doi.org/10.1126/scitranslmed.3009027
14. Eisner DA, Caldwell JL, Kistamás K, Trafford AW (2017) Calcium and excitation-contraction coupling in the heart. Circ Res 121:181–195. https://doi.org/10.1161/CIRCRESAHA.117.310230
15. Fakuade FE, Steckmeister V, Seibertz F, Gronwald J, Kestel S, Menzel J, Pronto JRD, Taha K, Haghighi F, Kensah G, Pearman CM, Wiedmann F, Teske AJ, Schmidt C, Dibb KM, El-Essawi A, Danner BC, Baraki H, Schwappach B, Kutschka I, Mason FE, Voigt N (2021) Altered atrial cytosolic calcium handling contributes to the development of postoperative atrial fibrillation. Cardiovasc Res 117:1790–1801. https://doi.org/10.1093/cvr/cvaa162
16. Florea SM, Blatter LA (2012) Regulation of cardiac alternans by β-adrenergic signaling pathways. Am J Physiol-Heart Circul Physiol 303:H1047-1056. https://doi.org/10.1152/ajpheart.00384.2012
17. Fraysse B, Weinberger F, Bardswell SC, Cuello F, Vignier N, Geertz B, Starbatty J, Krämer E, Coirault C, Eschenhagen T, Kentish JC, Avkiran M, Carrier L (2012) Increased myofilament Ca^{2+} sensitivity and diastolic dysfunction as early consequences of Mybpc3 mutation in heterozygous knock-in mice. J Mol Cell Cardiol 52:1299–1307. https://doi.org/10.1016/j.yjmcc.2012.03.009
18. Ganesh SK, Arnett DK, Assimes TL, Basson CT, Chakravarti A, Ellinor PT, Engler MB, Goldmuntz E, Herrington DM, Hershberger RE, Hong Y, Johnson JA, Kittner SJ, McDermott DA, Meschia JF, Mestroni L, O'Donnell CJ, Psaty BM, Vasan RS, Ruel M, Shen W-K, Terzic A, Waldman SA (2013) Genetics and genomics for the prevention and treatment of cardiovascular disease: update. Circulation 128:2813–2851. https://doi.org/10.1161/01.cir.0000437913.98912.1d
19. Heijman J, Molina CE, Voigt N (2018) Voltage-gated calcium channels and their roles in cardiac electrophysiology. In: Thomas D, Remme CA (eds) Channelopathies in heart disease. Springer International Publishing, Cham, pp 77–96
20. Huke S, Knollmann BC (2010) Increased myofilament Ca^{2+}-sensitivity and arrhythmia susceptibility. J Mol Cell Cardiol 48:824–833. https://doi.org/10.1016/j.yjmcc.2010.01.011
21. Hwang HS, Kryshtal DO, Feaster TK, Sánchez-Freire V, Zhang J, Kamp TJ, Hong CC, Wu JC, Knollmann BC (2015) Comparable calcium handling of human iPSC-derived cardiomyocytes generated by multiple laboratories. J Mol Cell Cardiol 85:79–88. https://doi.org/10.1016/j.yjmcc.2015.05.003
22. Itzhaki I, Maizels L, Huber I, Zwi-Dantsis L, Caspi O, Winterstern A, Feldman O, Gepstein A, Arbel G, Hammerman H, Boulos M, Gepstein L (2011) Modelling the long QT syndrome with induced pluripotent stem cells. Nature 471:225–229. https://doi.org/10.1038/nature09747
23. Itzhaki I, Rapoport S, Huber I, Mizrahi I, Zwi-Dantsis L, Arbel G, Schiller J, Gepstein L (2011) Calcium handling in human induced pluripotent stem cell derived cardiomyocytes. PLoS ONE 6:e18037. https://doi.org/10.1371/journal.pone.0018037
24. Katrukha IA (2013) Human cardiac troponin complex. Structure and functions. Biochem Mosc 78:1447–1465. https://doi.org/10.1134/S0006297913130063
25. Kim C, Wong J, Wen J, Wang S, Wang C, Spiering S, Kan NG, Forcales S, Puri PL, Leone TC, Marine JE, Calkins H, Kelly DP, Judge DP, Chen H-SV (2013) Studying arrhythmogenic right ventricular dysplasia with patient-specific iPSCs. Nature 494:105–110. https://doi.org/10.1038/nature11799
26. Knollmann BC, Potter JD (2001) Altered regulation of cardiac muscle contraction by troponin T mutations that cause familial hypertrophic cardiomyopathy. Trends Cardiovasc Med 11:206–212. https://doi.org/10.1016/S1050-1738(01)00115-3
27. Kumar S, Stevenson WG, John RM (2015) Arrhythmias in dilated cardiomyopathy. Card Electrophysiol Clin 7:221–233. https://doi.org/10.1016/j.ccep.2015.03.005
28. Kwak SG, Kim JH (2017) Central limit theorem: the cornerstone of modern statistics. Korean J Anesthesiol 70:144–156. https://doi.org/10.4097/kjae.2017.70.2.144
29. Lan F, Lee AS, Liang P, Sanchez-Freire V, Nguyen PK, Wang L, Han L, Yen M, Wang Y, Sun N, Abilez OJ, Hu S, Ebert AD, Navarrete EG, Simmons CS, Wheeler M, Pruitt B, Lewis R, Yamaguchi Y, Ashley EA, Bers DM, Robbins RC, Longaker MT, Wu JC (2013) Abnormal calcium handling properties underlie familial hypertrophic cardiomyopathy pathology in patient-specific induced pluripotent stem cells. Cell Stem Cell 12:101–113. https://doi.org/10.1016/j.stem.2012.10.010
30. Landstrom AP, Dobrev D, Wehrens XHT (2017) Calcium signaling and cardiac arrhythmias. Circ Res 120:1969–1993. https://doi.org/10.1161/CIRCRESAHA.117.310083
31. Law ML, Cohen H, Martin AA, Angulski ABB, Metzger JM (2020) Dysregulation of calcium handling in Duchenne muscular dystrophy-associated dilated cardiomyopathy: mechanisms and experimental therapeutic strategies. J Clin Med 9:520. https://doi.org/10.3390/jcm9020520
32. Lee Y-K, Ng K-M, Lai W-H, Chan Y-C, Lau Y-M, Lian Q, Tse H-F, Siu C-W (2011) Calcium homeostasis in human induced pluripotent stem cell-derived cardiomyocytes. Stem Cell Rev Rep 7:976–986. https://doi.org/10.1007/s12015-011-9273-3
33. Li Z, Chen P, Li C, Tan L, Xu J, Wang H, Sun Y, Wang Y, Zhao C, Link MS, Wilde AAM, Wang DW, Wang DW (2020) Genetic arrhythmias complicating patients with dilated cardiomyopathy. Heart Rhythm 17:305–312. https://doi.org/10.1016/j.hrthm.2019.09.012
34. Lian X, Hsiao C, Wilson G, Zhu K, Hazeltine LB, Azarin SM, Raval KK, Zhang J, Kamp TJ, Palecek SP (2012) Robust cardiomyocyte differentiation from human pluripotent stem cells via temporal modulation of canonical Wnt signaling. Proc Natl Acad Sci U S A 109:E1848–E1857. https://doi.org/10.1073/pnas.1200250109
35. Lian X, Zhang J, Azarin SM, Zhu K, Hazeltine LB, Bao X, Hsiao C, Kamp TJ, Palecek SP (2013) Directed cardiomyocyte differentiation from human pluripotent stem cells by modulating Wnt/β-catenin signaling under fully defined conditions. Nat Protoc 8:162–175. https://doi.org/10.1038/nprot.2012.150
36. Limas CJ, Olivari M-T, Goldenberg IF, Levine TB, Benditt DG, Simon A (1987) Calcium uptake by cardiac sarcoplasmic reticulum in human dilated cardiomyopathy. Cardiovasc Res 21:601–605. https://doi.org/10.1093/cvr/21.8.601
37. Liu G-S, Morales A, Vafiadaki E, Lam CK, Cai W-F, Haghighi K, Adly G, Hershberger RE, Kranias EG (2015) A novel human R25C-phospholamban mutation is associated with super-inhibition of calcium cycling and ventricular arrhythmia. Cardiovasc Res 107:164–174. https://doi.org/10.1093/cvr/cvv127
38. Malik FI, Hartman JJ, Elias KA, Morgan BP, Rodriguez H, Brejc K, Anderson RL, Sueoka SH, Lee KH, Finer JT, Sakowicz R, Baliga R, Cox DR, Garard M, Godinez G, Kawas R, Kraynack E, Lenzi D, Lu PP, Muci A, Niu C, Qian X, Pierce DW, Pokrovskii M, Suehiro I, Sylvester S, Tochimoto T, Valdez C, Wang W, Katori T, Kass DA, Shen Y-T, Vatner SF, Morgans DJ (2011) Cardiac myosin activation: a potential therapeutic

approach for systolic heart failure. Science 331:1439–1443. https://doi.org/10.1126/science.1200113
39. Malkovskiy AV, Ignatyeva N, Dai Y, Hasenfuss G, Rajadas J, Ebert AD (2020) Integrated Ca^{2+} flux and AFM force analysis in human iPSC-derived cardiomyocytes. Biol Chem 402:113–121. https://doi.org/10.1515/hsz-2020-0212
40. McCrohon JA, Moon JCC, Prasad SK, McKenna WJ, Lorenz CH, Coats AJS, Pennell DJ (2003) Differentiation of heart failure related to dilated cardiomyopathy and coronary artery disease using gadolinium-enhanced cardiovascular magnetic resonance. Circulation 108:54–59. https://doi.org/10.1161/01.CIR.0000078641.19365.4C
41. McKenna WJ, Maron BJ, Gaetano T (2017) Classification, epidemiology, and global burden of cardiomyopathies. Circ Res 121:722–730. https://doi.org/10.1161/CIRCRESAHA.117.309711
42. McNally EM, Mestroni L (2017) Dilated cardiomyopathy: genetic determinants and mechanisms. Circ Res 121:731–748. https://doi.org/10.1161/CIRCRESAHA.116.309396
43. Meyer M, Schillinger W, Pieske B, Holubarsch C, Heilmann PH, Kuwajima G, Mikoshiba K, Just H, Hasenfuss G (1995) Alterations of sarcoplasmic reticulum proteins in failing human dilated cardiomyopathy. Circulation 92:778–784. https://doi.org/10.1161/01.CIR.92.4.778
44. Moretti A, Bellin M, Welling A, Jung CB, Lam JT, Bott-Flügel L, Dorn T, Goedel A, Höhnke C, Hofmann F, Seyfarth M, Sinnecker D, Schömig A, Laugwitz K-L (2010) Patient-specific induced pluripotent stem-cell models for long-QT syndrome. New Engl J Med 363:1397–1409. https://doi.org/10.1056/NEJMoa0908679
45. Nakano SJ, Walker JS, Walker LA, Li X, Du Y, Miyamoto SD, Sucharov CC, Garcia AM, Mitchell MB, Ambardekar AV, Stauffer BL (2019) Increased myocyte calcium sensitivity in end-stage pediatric dilated cardiomyopathy. Am J Physiol Heart Circ Physiol 317:H1221–H1230. https://doi.org/10.1152/ajpheart.00409.2019
46. Narayan SM, Bode F, Karasik PL, Franz MR (2002) Alternans of atrial action potentials during atrial flutter as a precursor to atrial fibrillation. Circulation 106:1968–1973. https://doi.org/10.1161/01.cir.0000037062.35762.b4
47. Negretti N, Varro A, Eisner DA (1995) Estimate of net calcium fluxes and sarcoplasmic reticulum calcium content during systole in rat ventricular myocytes. J Physiol 486:581–591. https://doi.org/10.1113/jphysiol.1995.sp020836
48. Olivotto I, Oreziak A, Barriales-Villa R, Abraham TP, Masri A, Garcia-Pavia P, Saberi S, Lakdawala NK, Wheeler MT, Owens A, Kubanek M, Wojakowski W, Jensen MK, Gimeno-Blanes J, Afshar K, Myers J, Hegde SM, Solomon SD, Sehnert AJ, Zhang D, Li W, Bhattacharya M, Edelberg JM, Waldman CB, Lester SJ, Wang A, Ho CY, Jacoby D, EXPLORER-HCM study investigators (2020) Mavacamten for treatment of symptomatic obstructive hypertrophic cardiomyopathy (EXPLORER-HCM): a randomised, double-blind, placebo-controlled, phase 3 trial. Lancet 396:759–769. https://doi.org/10.1016/S0140-6736(20)31792-X
49. Papp Z, Agostoni P, Alvarez J, Bettex D, Bouchez S, Brito D, Černý V, Comin-Colet J, Crespo-Leiro MG, Delgado JF, Édes I, Eremenko AA, Farmakis D, Fedele F, Fonseca C, Fruhwald S, Girardis M, Guarracino F, Harjola V-P, Heringlake M, Herpain A, Heunks LM, Husebye T, Ivancan V, Karason K, Kaul S, Kivikko M, Kubica J, Masip J, Matskeplishvili S, Mebazaa A, Nieminen MS, Oliva F, Papp J-G, Parissis J, Parkhomenko A, Põder P, Pölzl G, Reinecke A, Ricksten S-E, Riha H, Rudiger A, Sarapohja T, Schwinger RH, Toller W, Tritapepe L, Tschöpe C, Wikström G, von Lewinski D, Vrtovec B, Pollesello P (2020) Levosimendan efficacy and safety: 20 years of SIMDAX in clinical use. Card Fail Rev. https://doi.org/10.15420/cfr.2020.03
50. Pearman CM (2014) An Excel-based implementation of the spectral method of action potential alternans analysis. Physiol Rep 2:e12194. https://doi.org/10.14814/phy2.12194
51. Pearman CM, Madders GWP, Radcliffe EJ, Kirkwood GJ, Lawless M, Watkins A, Smith CER, Trafford AW, Eisner DA, Dibb KM (2018) Increased vulnerability to atrial fibrillation is associated with increased susceptibility to alternans in old sheep. J Am Heart Assoc 7:e009972. https://doi.org/10.1161/JAHA.118.009972
52. Peper J, Kownatzki-Danger D, Weninger G, Seibertz F, Pronto JRD, Sutanto H, Pacheu-Grau D, Hindmarsh R, Brandenburg S, Kohl T, Hasenfuss G, Gotthardt M, Rog-Zielinska EA, Wollnik B, Rehling P, Urlaub H, Wegener J, Heijman J, Voigt N, Cyganek L, Lenz C, Lehnart SE (2021) Caveolin3 stabilizes McT1-mediated lactate/proton transport in cardiomyocytes. Circ Res 128:102–120. https://doi.org/10.1161/CIRCRESAHA.119.316547
53. Powers FM, Solaro RJ (1995) Caffeine alters cardiac myofilament activity and regulation independently of Ca^{2+} binding to troponin C. Am J Physiol 268:C1348-1353. https://doi.org/10.1152/ajpcell.1995.268.6.C1348
54. Rao C, Prodromakis T, Kolker L, Chaudhry UAR, Trantidou T, Sridhar A, Weekes C, Camelliti P, Harding SE, Darzi A, Yacoub MH, Athanasiou T, Terracciano CM (2013) The effect of microgrooved culture substrates on calcium cycling of cardiac myocytes derived from human induced pluripotent stem cells. Biomaterials 34:2399–2411. https://doi.org/10.1016/j.biomaterials.2012.11.055
55. Roberts WC, Siegel RJ, McManus BM (1987) Idiopathic dilated cardiomyopathy: analysis of 152 necropsy patients. Am J Cardiol 60:1340–1355. https://doi.org/10.1016/0002-9149(87)90618-7
56. Rougier J-S, Abriel H (2016) Cardiac voltage-gated calcium channel macromolecular complexes. Biochim Biophys Acta, Mol Cell Res 1863:1806–1812. https://doi.org/10.1016/j.bbamcr.2015.12.014
57. Schober T, Huke S, Venkataraman R, Gryshchenko O, Kryshtal D, Hwang HS, Baudenbacher F, Knollmann BC (2012) Myofilament Ca sensitization increases cytosolic Ca binding affinity, alters intracellular Ca homeostasis, and causes pause-dependent Ca-triggered arrhythmia. Circ Res 111:170–179. https://doi.org/10.1161/CIRCRESAHA.112.270041
58. Seibertz F, Reynolds M, Voigt N (2020) Single-cell optical action potential measurement in human induced pluripotent stem cell-derived cardiomyocytes. J Vis Exp. https://doi.org/10.3791/61890
59. Smith GL, Eisner DA (2019) Calcium buffering in the heart in health and disease. Circulation 139:2358–2371. https://doi.org/10.1161/CIRCULATIONAHA.118.039329
60. Sommese RF, Nag S, Sutton S, Miller SM, Spudich JA, Ruppel KM (2013) Effects of troponin T cardiomyopathy mutations on the calcium sensitivity of the regulated thin filament and the actomyosin cross-bridge kinetics of human β-cardiac myosin. PLoS ONE. https://doi.org/10.1371/journal.pone.0083403
61. Stevens CM, Rayani K, Singh G, Lotfalisalmasi B, Tieleman DP, Tibbits GF (2017) Changes in the dynamics of the cardiac troponin C molecule explain the effects of Ca^{2+}-sensitizing mutations. J Biol Chem 292:11915–11926. https://doi.org/10.1074/jbc.M116.770776
62. Stroik DR, Ceholski DK, Bidwell PA, Mleczko J, Thanel PF, Kamdar F, Autry JM, Cornea RL, Thomas DD (2020) Viral expression of a SERCA2a-activating PLB mutant improves calcium cycling and synchronicity in dilated cardiomyopathic hiPSC-CMs. J Mol Cell Cardiol 138:59–65. https://doi.org/10.1016/j.yjmcc.2019.11.147
63. Sun N, Yazawa M, Liu J, Han L, Sanchez-Freire V, Abilez OJ, Navarrete EG, Hu S, Wang L, Lee A, Pavlovic A, Lin S, Chen R, Hajjar RJ, Snyder MP, Dolmetsch RE, Butte MJ, Ashley EA, Longaker MT, Robbins RC, Wu JC (2012) Patient-specific induced pluripotent stem cells as a model for familial dilated cardiomyopathy. Sci Transl Med 4:130ra47-130ra47. https://doi.org/10.1126/scitranslmed.3003552

64. Thomas D, Christ T, Fabritz L, Goette A, Hammwöhner M, Heijman J, Kockskämper J, Linz D, Odening KE, Schweizer PA, Wakili R, Voigt N (2019) German Cardiac Society Working Group on Cellular Electrophysiology state-of-the-art paper: impact of molecular mechanisms on clinical arrhythmia management. Clin Res Cardiol 108:577–599. https://doi.org/10.1007/s00392-018-1377-1
65. Towbin JA, Lorts A (2011) Arrhythmias and dilated cardiomyopathy common pathogenetic pathways? J Am Coll Cardiol 57:2169–2171. https://doi.org/10.1016/j.jacc.2010.11.061
66. Trafford AW, Díaz ME, Eisner DA (1999) A novel, rapid and reversible method to measure Ca buffering and time-course of total sarcoplasmic reticulum Ca content in cardiac ventricular myocytes. Pflugers Arch 437:501–503. https://doi.org/10.1007/s004240050808
67. Trafford AW, Díaz ME, Negretti N, Eisner DA (1997) Enhanced Ca^{2+} current and decreased Ca^{2+} efflux restore sarcoplasmic reticulum Ca^{2+} content after depletion. Circ Res 81:477–484. https://doi.org/10.1161/01.res.81.4.477
68. van der Velden J, Merkus D, Klarenbeek BR, James AT, Boontje NM, Dekkers DHW, Stienen GJM, Lamers JMJ, Duncker DJ (2004) Alterations in myofilament function contribute to left ventricular dysfunction in pigs early after myocardial infarction. Circ Res 95:e85-95. https://doi.org/10.1161/01.RES.0000149531.02904.09
69. van der Velden J, Papp Z, Zaremba R, Boontje NM, de Jong JW, Owen VJ, Burton PBJ, Goldmann P, Jaquet K, Stienen GJM (2003) Increased Ca^{2+}-sensitivity of the contractile apparatus in end-stage human heart failure results from altered phosphorylation of contractile proteins. Cardiovasc Res 57:37–47. https://doi.org/10.1016/s0008-6363(02)00606-5
70. Voigt N, Heijman J, Wang Q, Chiang DY, Li N, Karck M, Wehrens XHT, Nattel S, Dobrev D (2014) Cellular and molecular mechanisms of atrial arrhythmogenesis in patients with paroxysmal atrial fibrillation. Circulation 129:145–156. https://doi.org/10.1161/CIRCULATIONAHA.113.006641
71. Voigt N, Li N, Wang Q, Wang W, Trafford AW, Abu-Taha I, Sun Q, Wieland T, Ravens U, Nattel S, Wehrens XHT, Dobrev D (2012) Enhanced sarcoplasmic reticulum Ca^{2+} leak and increased Na^{+}-Ca^{2+} exchanger function underlie delayed afterdepolarizations in patients with chronic atrial fibrillation. Circulation 125:2059–2070. https://doi.org/10.1161/CIRCULATIONAHA.111.067306
72. Wang L, Kryshtal DO, Kim K, Parikh S, Cadar AG, Bersell KR, He H, Pinto JR, Knollmann BC (2017) Myofilament Ca-buffering dependent action potential triangulation in human iPSC model of hypertrophic cardiomyopathy. J Am Coll Cardiol 70:2600–2602. https://doi.org/10.1016/j.jacc.2017.09.033
73. Weiss JN, Nivala M, Garfinkel A, Qu Z (2011) Alternans and arrhythmias: from cell to heart. Circ Res 108:98–112. https://doi.org/10.1161/CIRCRESAHA.110.223586
74. Wolff MR, Buck SH, Stoker SW, Greaser ML, Mentzer RM (1996) Myofibrillar calcium sensitivity of isometric tension is increased in human dilated cardiomyopathies: role of altered beta-adrenergically mediated protein phosphorylation. J Clin Invest 98:167–176. https://doi.org/10.1172/JCI118762
75. Wolff MR, Whitesell LF, Moss RL (1995) Calcium sensitivity of isometric tension is increased in canine experimental heart failure. Circ Res 76:781–789. https://doi.org/10.1161/01.RES.76.5.781
76. Wu H, Lee J, Vincent LG, Wang Q, Gu M, Lan F, Churko JM, Sallam KI, Matsa E, Sharma A, Gold JD, Engler AJ, Xiang YK, Bers DM, Wu JC (2015) Epigenetic regulation of phosphodiesterases 2A and 3A underlies compromised β-adrenergic signaling in an iPSC model of dilated cardiomyopathy. Cell Stem Cell 17:89–100. https://doi.org/10.1016/j.stem.2015.04.020
77. Yazawa M, Hsueh B, Jia X, Pasca AM, Bernstein JA, Hallmayer J, Dolmetsch RE (2011) Using induced pluripotent stem cells to investigate cardiac phenotypes in Timothy syndrome. Nature 471:230–234. https://doi.org/10.1038/nature09855
78. Zhang X-H, Haviland S, Wei H, Šarić T, Fatima A, Hescheler J, Cleemann L, Morad M (2013) Ca^{2+} signaling in human induced pluripotent stem cell-derived cardiomyocytes (iPS-CM) from normal and catecholaminergic polymorphic ventricular tachycardia (CPVT)-afflicted subjects. Cell Calcium 54:57–70. https://doi.org/10.1016/j.ceca.2013.04.004